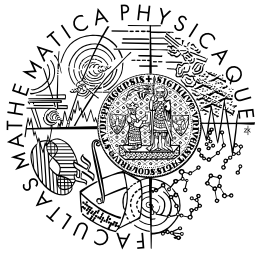

FACULTY
OF MATHEMATICS
AND PHYSICS
Charles University

MASTER THESIS

Eliška Šestáková

Spectroscopic study of temperature-sensitive hydrogels

Department of Macromolecular Physics

Supervisor of the master thesis:	doc. RNDr. Lenka Hanyková, Dr.
Study programme:	Physics
Study branch:	Biophysics and Chemical Physics

Prague 2019

I declare that I carried out this master thesis independently, and only with the cited sources, literature and other professional sources.

I understand that my work relates to the rights and obligations under the Act No. 121/2000 Sb., the Copyright Act, as amended, in particular the fact that the Charles University has the right to conclude a license agreement on the use of this work as a school work pursuant to Section 60 subsection 1 of the Copyright Act.

In ..... date ..... signature of the author

I would like to thank to my supervisor, doc. RNDr. Lenka Hanyková, Dr., whose experiences, advice and suggestions were invaluable. I really appreciate the kind and helpful attitude. I would also like to express my thanks to doc. RNDr. Ivan Krakovský, CSc. for the instruction and help during the preparation and swelling measurements.

I am very grateful to my closest family and friends for the support, encouragement and patience throughout my study.

Title: Spectroscopic study of temperature-sensitive hydrogels

Author: Eliška Šestáková

Department: Department of Macromolecular Physics

Supervisor: doc. RNDr. Lenka Hanyková, Dr., Department of Macromolecular Physics

Abstract: Polymer hydrogels are materials composed of the polymer network, which have the ability to swell in water-based solutions. The temperature change can induce a phase transition in some of the hydrogels. The hydrogel shrinks and the solvent is released. The phase transition is called the collapse and it is caused by the microscopic coil-globule transition. In this thesis, the phase transition of the single (PDEAAm) and double network hydrogels (PDEAAm/PAAm, PDEAAm/PDMAAm) was studied with swelling experiments, NMR spectroscopy and UV-Vis spectrocopy. One of the main results is that the second and hydrophilic component causes the broader temperature interval and decreases the extent (enthalpy and entropy) of the collapse. It was proved that the cross-linking density of the first hydrogel network does not affect the collapse, but it influences the final composition of the double network hydrogels during the preparation. The spin-spin relaxation time measurements demonstrate bound water existence only in the single network systems. The double network systems are probably heterogeneous, expecially PDEAAm/PAAm samples have a strongly porous structure. Measuring drug model release, the exponential decay of the swollen solution in the hydrogel was proved.

Keywords: hydrogels, phase transition, NMR spectroscopy

Contents

Introduction **3**

1 Hydrogels **4**
1.1 Hydrogels research 5
1.2 Hydrogels around us 6
1.2.1 Natural hydrogels 6
1.2.2 Hydrogels application 6
1.3 Temperature-sensitive hydrogels 9
1.4 Double network hydrogels 9
1.5 PDEAAm research 10

2 Experimental techniques **12**
2.1 Swelling experiments 12
2.2 NMR spectroscopy 12
2.2.1 Physical basis 13
2.2.2 Chemical shift 15
2.2.3 CPMG sequence 16
2.3 UV-Vis spectroscopy 17

3 Goals of the thesis **18**

4 Preparation **19**
4.1 Single networks 19
4.2 Double networks 20

5 Measurement and results **22**
5.1 Swelling experiments 22
5.1.1 Extent of swelling 23
5.1.2 Parameters of collapse 24
5.2 NMR spectra 27
5.2.1 Measured spectra 28
5.2.2 Temperature dependency 30
5.3 NMR relaxation experiments 32
5.4 UV-Vis spectroscopy 34

6 Discussion **41**
6.1 Swelling experiments 41
6.2 NMR - temperature dependency 42
6.3 NMR - spin-spin relaxation time measurement 43
6.4 UV-Vis spectroscopy 44

Conclusion **45**

Bibliography **47**

List of Figures **50**

List of Tables **52**

Introduction

Polymer hydrogels are materials that have been found very useful in many application of everyday life as well as they have a great potentiality of use in biotechnologies and medicine [1]. They are composed of a polymer network, which have the ability to swell in water-based solutions. An interesting consequence of the polymer network amphiphilic character is the stimuli responsiveness. A temperature change can induce a phase transition when a hydrogel shrinks and solvent is released. The concept of double network hydrogels is a unique way how to get tougher materials in comparison with the single network hydrogels.

In this thesis, we prepared thermoresponsive polymer hydrogels and examined their behaviour during the temperature induced phase transition. Single network (SN) and double network (DN) hydrogels were prepared with a various network density. As the first network, poly-N, N'-diethylacrylamide (PDEAAm) was used and polyacrylamide (PAAm) and poly-N, N'-dimethylacrylamide (PDMAAm) as the second one. Properties of the samples were examined with several experimental methods, such as swelling experiments, nuclear magnetic spectroscopy (NMR) and ultraviolet-visible spectroscopy (UV-Vis).

The NMR spectra and swelling experiments are focused on the parameters of the collapse, such as enthalpy, entropy, critical temperature and temperature interval of the collapse. These two methods are qualitatively very different, the results are gained in both macroscopic and microscopic way. The NMR relaxation experiments and UV-Vis spectroscopy study the water molecules swollen in the samples and the dynamics and flexibility. NMR relaxations show us the matter on the microscopical level again and UV-Vis demonstrate the release behaviour in possible applications.

1. Hydrogels

Hydrogels are polymer networks that tend to swell in water based solutions. It means that the water molecules are bound to the structure by hydrogen bonds mainly. According to the origin, hydrogels can be divided into synthetic or natural.

A dried out hydrogel is usually opaque, white coloured and quite fragile. It increases the volume many times after swelling, it becomes transparent, even limpid. A dried out and swollen hydrogel is depicted in figure 1.1.

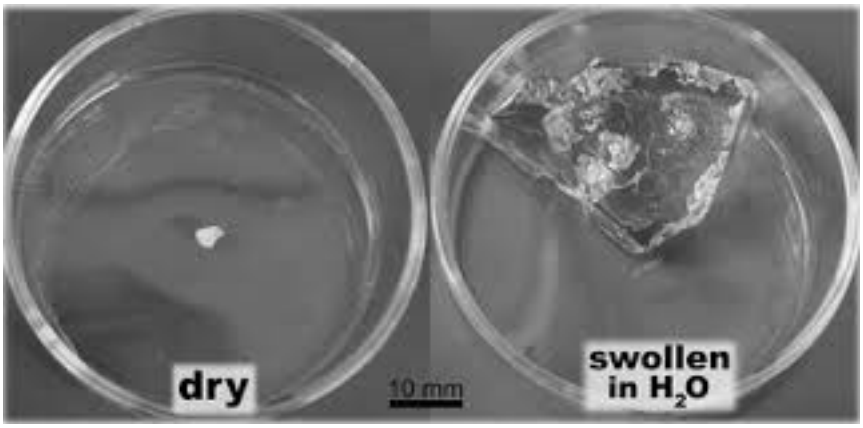

Figure 1.1: Hydrogel sample dried out (left) and swollen (right), [2]

The hydrogels consist of a polymer, the substance composed of monomer units connected into chains. The chains can also connect to each other physically (e.g. UV radiation) or chemically (cross-linker) and create the polymer network. The polymer network bonds the water molecules to its structure mainly by hydrogen bonds. The model of the swollen polymer network is shown in figure 1.2. The red circled points of the polymer chains are called the junctions.

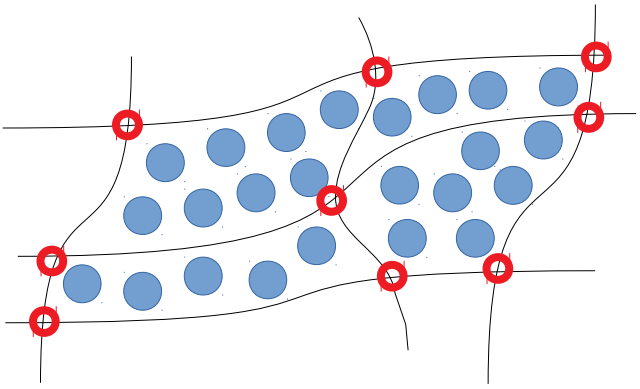

Figure 1.2: Model of polymer network swollen in water

1.1 Hydrogels research

The hydrogels research can be divided into several epochs according to the main aims of the interest:

First generation

The first cross-linked network material, which has all the properties of the hydrogel was described in 1960, [3]. The materials were ment to be used for biological applications and to be in contact with a living tissue. Finally, the research lead to the invention of soft contact lenses.

The research was focused on quite simple materials with a potential of a biotechnological use then. It studies chemically cross-linked polymers such as PHEMA, poly(vinyl alcohol) (PVA) and poly(ethylene glycol) (PEG).

Second generation

In the beginning of the 1970s, the aim of interest shifted to hydrogels, which are able to react to surrounding changes, e.g. temperature, pH, the presence of a substance in water solution. This feature is caused by the conformational change inducting a phase transition. Temperature-sensitive hydrogels are the most examined. Especially temperature-sensitive gelation hydrogels have an advantage of injecting as *in situ* forming system reaching the required shape in a body cavity. The process is a minimally invasive and without demanding surgery procedures. Hydrogels containing poly(*N*-isopropylacrylamide) PNIPAAm are widely investigated.

Third generation

In the 1990s, new physical ways of the cross-linking are investigated except for already used hydrophobic and ionic interactions. It could provides better mechanical strength and other needed hydrogel properties. E.g., inclusion complex formation, metal-ligand coordination and peptide interactions are examined for hydrogels preparation.

Smart hydrogels

In the last phase of hydrogels research, smart hydrogels are studied. They are chemically cross-linked hydrogel with a possibility of various covalently bonded functional groups. The samples are also able to respond to multiple triggers due to the proper modification and multi-component content. Some of the components can be temperature or pH-sensitive. A concept of double network hydrogels appears and provides much better mechanical properties of the hydrogels. The main interest of applications is still the biological use in tissue engineering, drug delivery and releasing, etc. The hydrogels of desirable properties for certain applications can be gained by a combination of all named varying methods. More information about the history of the hydrogel research is gathered in [4].

1.2 Hydrogels around us

1.2.1 Natural hydrogels

Hydrogels are not only synthetic but also natural. The natural hydrogels occur even in our bodies, e.g. fibrin, collagen and some polysaccharides.

All of them are very important for many basic functions. Fibrin creates network which covers wounds and creates a support capturing blood cells. The structure stops the bleeding and fibrin creates a continuous medium which is suitable for the tissue recovery inside and dries out outside creating a protection barrier.

There are many kinds of the collagen, each of them is necessary in specific tissues such as cartilages, tendons, muscles, joints and ligaments. All these structures are hardly replaceable and represent an area where the results of the hydrogels research might be used.

1.2.2 Hydrogels application

We are everyday in touch not even with natural hydrogels but also with synthetic hydrogels.

Diapers: Disposable diapers use the hydrogel ability of a fluids absorption. Polymer polyacrylate is used as the functional substance. The advantages of disposable diaper are that it absorbs even when it is already wet, it is dry on the surface even when swollen and it is saves your time and work. Diapers have many disadvantages though. There are doubts that it can cause health problems, e.g. rash, asthma, infertility and even cancer. All listed problems are consequences of the watertight and non-breathable plastic outer layer. The biggest problem about diapers is the huge quantity of producing waste, which is hardly disposable.

Plants Hydration: Hydrogels might be very helpful even for gardeners. Polyacrylamide based hydrogel beads absorb redundant water and release it during a dry season. The defect of the method is that the polymer is degraded into the monomer, which is toxic in contrast with the polymer. The purpose is the utilisation of biodegradable, natural hydrogels.

Some of the plants are able to grow only using the hydrogel beans, see figure 1.3.

Cosmetics: Hydrogels are often used in cosmetic preparations meant to hydrate the skin. There are many facial masks based on collagen, hyaluronic acid, etc. These masks are proclaimed to hydrate and cause an anti-aging effect and reduce wrinkles. Hydrogels are used even in mascaras, moisturizing creams and so on. The hydrogels frequent utilisation is caused by a low primary irritation index, which makes the testing of new products quicker. Due to the many ways of modification (cross-linking density, various additional substances), the properties of the tested and proved hydrogels can be easily changed for applications in different products.

Plastic surgery: Hydrogels are materials suitable for contact with the human body because of similar properties as many tissues. Hyaluronic acid can be used mostly as a tissue filling. It is widely used in plastic surgery, although it is often called as a controversial material. There are not enough studies, so it has been applied till nowadays in some tissues. Hyaluronic acid is banned from being

Figure 1.3: Plant cultivated with hydrogel beans

used as the filling in breasts because of the shielding during the mammography screening. Hyaluronic filling are still popular, e.g. in the lips, under the eyes and for nose shaping.

Environmental applications: The biggest problem of the last years is the water pollution. Hydrogels provide a manner how to face it. The problem can be partly solved using them in two ways. The first one is a hydrogel matrix capturing metal ions and other pollutants. Other possibility of the hydrogel use is a cultivating of microorganisms in the polymer network. Chlorella and Spirulina are the most used organisms, they are able to depurate surrounding water.

The most interesting application of the hydrogels is **medicine**. There are many branches, which finds the hydrogel as a potential helper, e.g. tissue engineering, bone regeneration, plastic surgery as mentioned above, wound dressing and ophthalmology.

Tissue engineering: Many patients have problem with damaged tissues, which are hardly replaceable and need problematic surgeries. The tissue engineering *in-vivo* combines the injectable hydrogesl and patients' stem cells, which are held *in-vitro* before it is ready to implant. The hydrogel behave as an extracellular matrix that supports a cell proliferation and regrowth, see figure 1.4. It enriched with growth factors, metabolites and other materials for a faster and successful treatment.

The hydrogels act as an environment perfect for the cell, metabolic transports. They can be easily modificated with ligands to change the properties. The hydrogels are also usually biodegradable, which is another advantage. In contradiction, the disadvantages of the hydrogels are paradoxically connected with the benefit, the tissue-like structure. It means that they might be difficult to handle, to sterilize and also mechanically weak and brittle (which could be fixed with the double networks).

The experiments of tissue engineering are being tested, not clinically used yet. The satisfying results could serve for the development of a synthetic extracellular matrix, self-shaping to fit the cavity, and for a simulation of physiologic micro

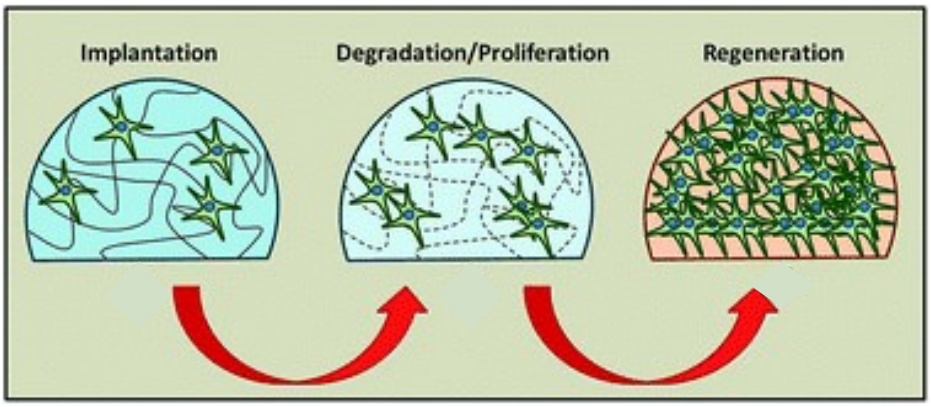

Figure 1.4: Hydrogel as extracellular matrix for cell cultivation, [5]

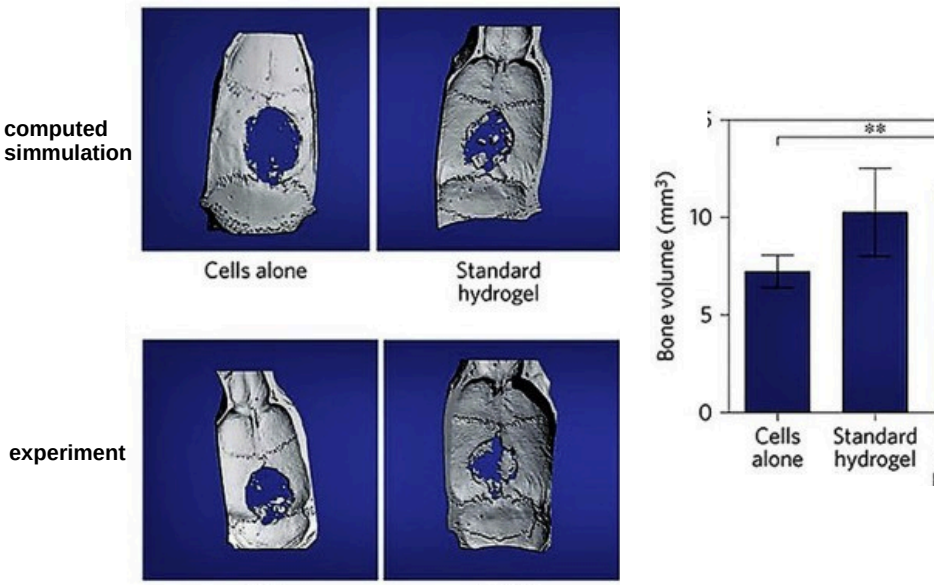

Figure 1.5: Bone regeneration of rat cranial deffect with and without hydrogel 12 weeks post-transplantation , [6]

environment for *in-vitro* experiments avoiding an animal testing. The research is currently focused on the natural hydrogels, such as gelatin (denatured collagen), chitosan, hyaluronic acid, pectin and alginate.

One of the examples of the tissue engineering is the bone regeneration. In figure 1.5, the cell-hydrogen matrix was transplanted to the rat cranial defect. The upper figures show a computed assumption while in the lower figures, results of the experiment after 12 weeks after the transplantation are depicted. It is obvious that the new bone volume is bigger in the case of using the hydrogel (right) than using only the cell. The feature is also demonstrated in the graph on the right side.

Drug delivery: Another possible utilisation of the smart hydrogels particularly is in the drug delivery transport. Standard methods fight with a quick release of the healing substance and efficiency decrease. The substance swollen in a hydrogel diffuses very slowly and can be release by a trigger, a temperature or pH change that happens in a diseased tissue.

Wound dressing The hydrogels are widely used for a wound dressing. They are used not only for small injuries, such as blisters, but also for more serious wounds, such as large burns. They behave as "the second skin", they perfectly adhere the skin, adapt the shape and keep the skin from an abrasion.

The great potential of the hydrogels cannot be doubted. We can find them at easy and clever applications of everyday life as well as at sophisticated uses in medicine and research.

More information about the mentioned problematics are given by the references gathered in [1] or [7].

1.3 Temperature-sensitive hydrogels

In this thesis, temperature-sensitive hydrogels are studied. The hydrogels sensitive to the change of surrounding conditions are called the intelligent hydrogels. The sensitivity is demonstrated by the phase transition occurence on the microscopic level. The phase transition is called a collapse. There are several factors that can induce the collapse, such as pH, temperature or the presence of certain chemical substances.

The temperature-induced volume phase transition in a cross-linked hydrogels is a similar phenomenon as the phase separation in polymer solutions exhibiting a lower critical solution temperature (LCST). On the molecular level, both phase separation in solutions and volume phase transition in cross-linked hydrogels are assumed to be a macroscopic manifestation of a coil-globule transition [8]. This process is demonstrated in figure 1.6.

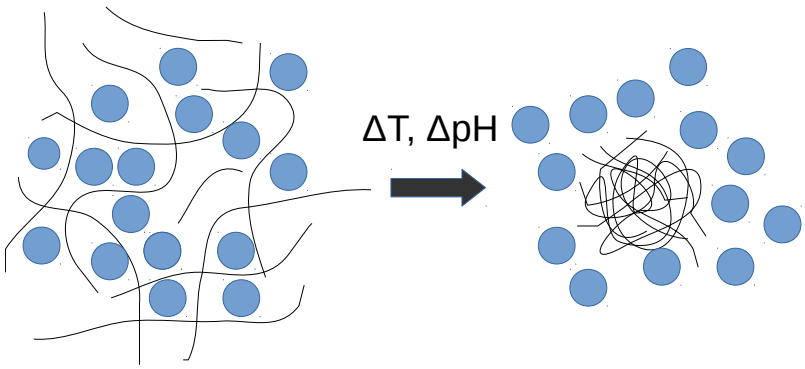

Figure 1.6: Structure change of free chains - globules inducting collapse

The temperature sensitivity is caused by the amphiphile character of the polymer units. As the temperature rises, the conformation of the free flexible polymer chains becomes less energetically favourable and the polymer chain packs into a globule. This conformational change induces the collapse. The collapse is connected with a water releasing out of the polymer structure.

1.4 Double network hydrogels

Single network hydrogels (SN) that are created only with one type of polymer have a limited temperature-sensitivity and possibility to enhance the collapse parameters. Methods leading to better temperature-sensitive properties are often

associated with a reduced mechanical strength. Interpenetrating polymer networks (IPN) combine two or more types of the polymer networks and give us a chance to tune the hydrogel parameters, such as the collapse behaviour, rate of swelling and mechanical properties. The IPN polymer networks are interlaced but they are not covalently bonded.

Double network (DN) hydrogels that are a special class of the IPN were introduced in [9] by Gong. The DN hydrogels are composed of two networks, the first one is densely cross-linked and the second one is cross-linked poorly. This scheme ensures a high rate of swelling and mechanical strength and toughness at the same time. This model has a great potential of the use because single networks created only with one polymer network are usually very brittle and unsuitable for many applications.

The first DN hydrogels were composed of poly(2-acrylamide-2-methyl-propane sulfonic acid) and polyacrylamide. The high toughness of the hydrogel was caused by internal fractures in the first network upon deformation, which acted as additional crosslinkers [10]. The DN hydrogels were formed from two biocompatible polymers, poly(vinyl alcohol) and poly(ethylene glycol) with a freezing and thawing method [11]. The hydrogels with various cross-linking density of the first network and the effect on the swelling and mechanical properties were studied, the toughness of the hydrogel was found to be proportional to the cross-linking of the first network [12].

Many other DN hydrogels have been investigated but only a few of them where temperature-sensitive.

DN PNIPAAm/PNIPAAm hydrogels with polysiloxane nanoparticles [13] or an ionized first network with a electrostatic comonomer [14] were studied. The influence of the hydrogel composition on the collapse, structure, swelling equilibrium, swelling kinetics and mechanical properties was described.

PNIPAAm is an abudantly studied and well-characterized polymer. Moreover, PNIPAAm critical temperature is in the physiologic range that makes him very popular. The application of PNIPAAm in contact with a human body evokes a potential release of toxic low-molecular-weight amines due to hydrolysis though. This is a cause why other temperature-sensitive polymers are proposed as alternatives for the bioapplications [15].

1.5 PDEAAm research

Poly(N, N'-diethylacrylamide) (PDEAAm) with volume phase transition temperature 304 – 307 K [16] is one of the PNIPAAm alternatives and seems to be suitable for the bioapplications, because cytotoxicity of PDEAAm hydrogels is less significant than for PNIPAAm hydrogels [17]. PDEAAm is an N-substituted temperature-sensitive polymer. PNIPAAm and PDEAAm have the same backbone structure but different N-substituted groups, two ethyl groups in PDEAAm and one isopropyl group in PNIPAAm. PDEAAm can only behaves as a hydrogen bond acceptor and thus disable the formation of intra- or interchain hydrogen bonds because of the absence of NH groups.

PDEAAm was investigated also with PNIPAAm in various solutions by photometry and high sensitivity differential scanning calorimetry (DSC). The salt

effect was found out to influence PNIPAAm and PDEAAm in the same way with decreasing the lower critical solution temperature [16].

The PDEAAm ability to store and release active agents was studied. It is an attractive candidate for the biomedical applications, drug delivery mainly. [18].

PDEAAm is often compared with PNIPAAm and it was found that the swelling properties of both hydrogels can be influenced with the cross-linking density. The swelling ratio of PDEAAm hydrogels below volume phase transition temperature is much lower than at the PNIPAAm hydrogels, which is caused by the different chemical structure of the side chains [19], [20]. PDEAAm has a stronger dependency on the cross-linking agent, slower reswelling kinetics and also broader temperature phase transition region.

The copolymerization of DEAAm with a hydrophilic monomer (or fixing another polymer into PDEAAm hydrogel) to form IPN were used to control the phase transition behaviour. The swelling properties and parameters of the phase transition were studied using NMR, Fourier transform infrared spectroscopy and modulated DSC [21].

2. Experimental techniques

At first, we practiced swelling experiments for a basic characterization of the samples. Then, we applied NMR spectroscopy to describe the collapse of the hydrogels by a microscopical method. Properties of the collapse gained from these methods can be qualitatively compared.

The swollen hydrogels contain a certain amount of water, which is released above the critical temperature. NMR spectroscopy relaxations and UV-Vis were applied to study the bound and free water in the samples.

2.1 Swelling experiments

The swelling experiments represent a simply but efficient method characterizing basic properties of hydrogels and their behaviour during the collapse. The advantages of this experimental method is a simplicity and the disadvantages are the accuracy and time-consuming character.

Swollen samples are immersed in distilled water and heated in the swelling experiments. The heating is quite slow, the phase transitions apears continuous and smooth. The samples are weighted and returned back to the warm solution. The result is the sample temperature dependency of the polymer mass. These experiments might be useful to specify the polymer and water fractions in the hydrogels. There are exchanges among these two kinds of molecules.

2.2 NMR spectroscopy

Nuclear magnetic resonance spectroscopy (NMR) is a method that operates with a nuclei of non-zero nuclear spin. ^{1}H and ^{13}C are the most commonly used isotopes, both of spin 1/2. Experiments can also includes other nuclei as ^{15}N, ^{19}F or ^{31}P.

The nuclear energy is quantized when a particle is settled in an outer magnetic field. It means that there are only a few energy values that correspond to the states in which the particle can be found. Transitions between energy levels can be induced by a radiofrequency pulse. The absorbed energy is detected and shown as a spectral line. The example of measured ^{1}H PDEAAm spectrum is depicted in figure 2.1. ^{1}H NMR spectrum provides many information about a measured sample, the most fundamental are, e.g:

- The spectral lines correspond to various protons of the molecule. The protons with the same chemical environments belong to one signal. This property is caused by a chemical shift, which will be discussed later.
- The area defined by a spectral line is proportional to the number of proton with the same chemical shift.
- Some of the spectral lines may be split and create multiplets, which is a consequence of the spin-spin coupling, magnetic interaction between the nuclei mediated through bonds.

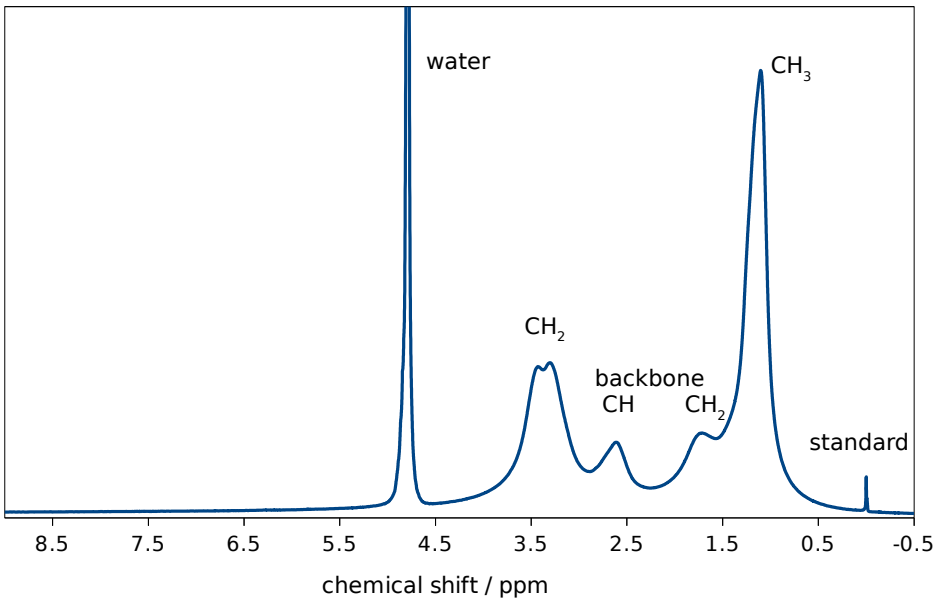

Figure 2.1: ^{1}H spectrum of poly(N, N'-diethylacrylamide)

2.2.1 Physical basis

An atom nucleus has got an intrinsic angular momentum, spin $\boldsymbol{I}$. The spin is always associated with magnetic dipole moment $\boldsymbol{\mu}$

$$\boldsymbol{\mu} = \gamma \boldsymbol{I}, \tag{2.1}$$

where γ stands for the gyromagnetic ratio that is specific for every nucleus.

The nuclear spin is quantized, it means that its magnitude is quantized as well as the x, y and z-components, e.g. when a magnetic field is applied, there are $2I + 1$ states for I_z expressed by

$$I_z = m\hbar, \tag{2.2}$$

where $\hbar$ is the reduced Planck constant and m is the magnetic quantum number, which can take values $-I, -I + 1, ..., I - 1, I$.

Thus, when the nucleus is situated in a magnetic field, there are $2I+1$ possible values of $\boldsymbol{\mu_z}$.

The energy of a magnetic dipole moment is expressed as

$$E = -\boldsymbol{\mu}.\boldsymbol{B_0}. \tag{2.3}$$

We choose $\boldsymbol{B_0}$ in the direction of z axis and get

$$E = -\boldsymbol{\mu}_z B_0 = -\gamma m \hbar B_0. \tag{2.4}$$

Hence, the nuclei with different spin states have different energies and different populations in the thermal equilibrium.

When considering a proton with spin $\dfrac{1}{2}$, there are two states, which are possible, states with magnetic quantum number $m = \pm\frac{1}{2}$. Unless a magnetic field is

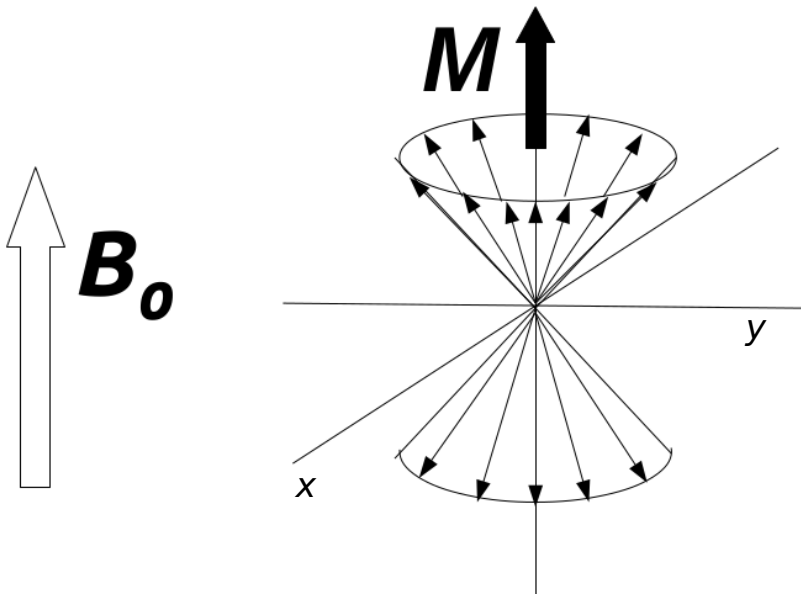

Figure 2.2: Model of magnetization in magnetic field B_0

applied, the proton energy is degenerated. The energy splitting onto two levels appears when a magnetic field is present and the energy difference is

$$\Delta E = \gamma \hbar B_0. \tag{2.5}$$

Magnetization $\boldsymbol{M}$ is a vector sum of all magnetic dipole moments, see figure 2.2. The magnetic dipole moments make a precession move around a conical surface. The magnetization is oriented according to the direction of more populated state (with lower energy). The magnetic dipole moments of more populated state are shown above the xy plane in this case. It is a macroscopic quantity, which can be handled and detected. The magnetization move is precessional around $\boldsymbol{B}$ field with the angular frequency

$$\omega = -\gamma B, \tag{2.6}$$

where B stands for the field magnitude. The precession of a magnetization, which was taken out of the equilibrium, happens in $\boldsymbol{B_0}$ field with the Larmor frequency

$$\omega_L = -\gamma B_0. \tag{2.7}$$

The NMR spectrometer studies the magnetization, which has been deflected by a radiofrequency pulse. Subsequently, the magnetization projection in xy plane is measured. The pulse induces a change in states populations, thus the magnetization is deflected and rotates around z axis with a frequency of the radiofrequency pulse. The frequency must be equal to γB_0 to excitate the system. The magnetization is relaxing after the end of the pulse and returns back to the initial position, inducting an oscillating current on the probe detection coil.

The magnetization in the presence of the radiofrequency pulse is described by the Bloch equations

$$\frac{dM_x(t)}{dt} = \gamma(\boldsymbol{M}(t) \times \boldsymbol{B}(t))_x - \frac{M_x(t)}{T_2}$$

$$\frac{dM_y(t)}{dt} = \gamma(\boldsymbol{M}(t) \times \boldsymbol{B}(t))_y - \frac{M_y(t)}{T_2} \tag{2.8}$$

$$\frac{dM_z(t)}{dt} = \gamma(\boldsymbol{M}(t) \times \boldsymbol{B}(t))_z - \frac{(M_z(t) - M_0)}{T_1} \ .$$

M_x, M_y, M_z stand for the components of the magnetization and M_0 is the magnetization magnitude before the pulse. $\boldsymbol{B}$ is the total magnetic field during the radiofrequency pulse application.

$$\boldsymbol{B} = (B_{rfx}, B_{rfy}, B_0) \tag{2.9}$$

T_1 is the longitudinal (or spin-lattice) relaxation time that describes the recovery of M_z. T_2 is called the transverse (or spin-spin) relaxation time, the constant corresponding to the decay of M_{xy}. After the end of the pulse ($t = 0$), the transverse magnetization acts according to formula

$$M_{xy}(t) = M_{xy}(0)e^{-t/T_2}. \tag{2.10}$$

An intensity dependency $I(\omega)$ can be reached solving the Bloch equations 2.8. The dependency is depicted in measured spectra and has a shape of the Lorentz curve.

2.2.2 Chemical shift

Different measured nuclei have a diverse value of the Larmor frequency. Considering the nuclei of the same isotope, the Larmor frequency is dependent on the local magnetic field. The local magnetic field is given by a superposition of static field B_0 and magnetic fields that are created by the electron shells of all measured and surrounding atoms. The local magnetic field is expressed as

$$B_{local} = B_0(1 - \sigma), \tag{2.11}$$

where σ is a constant of the magnetic shielding and includes many effects:

$$\sigma = \sigma_{dia} + \sigma_{para} + \sigma^{'}. \tag{2.12}$$

σ_{dia} is positive and corresponds to the shielding of σ electrons in s orbitals. Constant σ_{para} is negative and corresponds to the shielding of π orbitals. Constant $\sigma^{'}$ expresses the effect of the neighbour atoms.

The resonance frequency for nuclei with the same chemical environment equals

$$\omega = \gamma(1 - \sigma)B_0. \tag{2.13}$$

The frequency of a signal with the same chemical shift depends on the static magnetic field according to formula 2.13. That is the reason, why chemical shift δ with units ppm (parts per million) is defined. It holds

$$\delta[ppm] = \frac{\omega[Hz] - \omega_{standard}[Hz]}{\omega_{standard}[Hz]} 10^6, \tag{2.14}$$

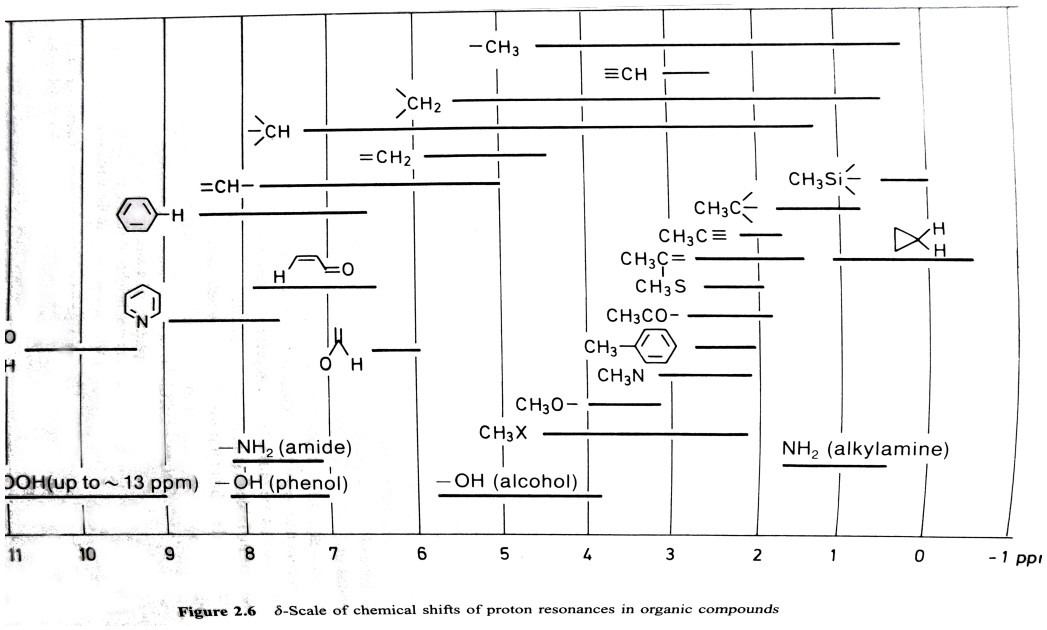

Figure 2.6 δ-Scale of chemical shifts of proton resonances in organic compounds

Figure 2.3: Proton chemical shift of function groups from organic solvents, [22]

where $\omega_{standard}$ is the resonance frequency of a standard that is a chemical substance whose signal is characterized by inertness to the changes of the temperature, pH etc.

A signal (which can be split into more peaks) belongs to the chemically equivalent nuclei, the nuclei of a certain function group. In figure 2.3, there are some of the most common function group of organic solvents with typical chemical shift δ.

2.2.3 CPMG sequence

The Carr-Purcell-Meiboom-Gill (CPMG) is a sequence used for T_2 (the transverse relaxation time) detection. It is a quite simple sequence, which is figured below in 2.4.

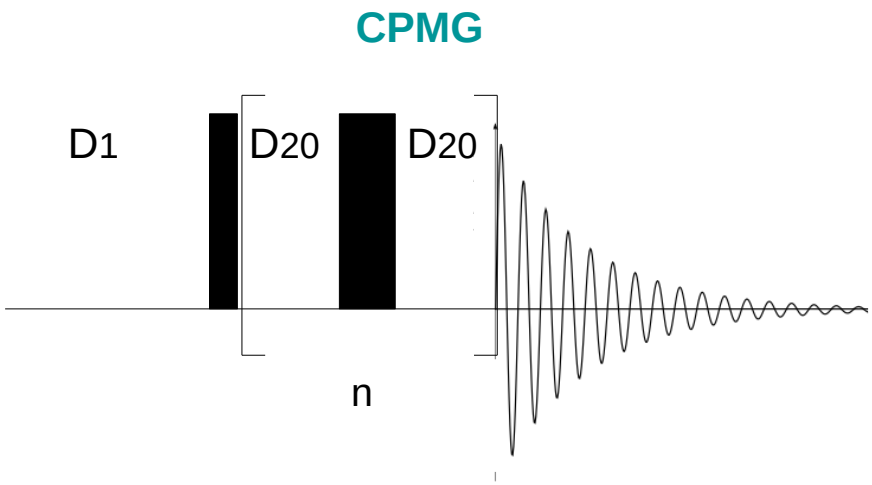

Figure 2.4: The CPMG sequence for T_2 measuring

The CPMG sequence is characterized with a few parameters, $D1, D20$ and n that specifies the number of repetition of the middle block in the brackets. The magnetization (in figure 2.2) is deflected by the first $\pi/2$ pulse to the xy plane after $D1$ time. The dipole moments (still in figure 2.2) in xy plane interact with each other during $D20$ delay and dephase. The π pulse rotate the spins into the other direction and the spins are phased again. This process is the basis of spin-echo and repeats n times. Finally, an acquisition is performed. The spin-spin relaxation time is reached with fitting measured set of data with 2.10.

Measuring the relaxation time is very useful, because molecules at various conditions show different dynamics, which is connected with the relaxation time. This feature is for example applied in magnetic resonance imaging using the fact that water in different tissues has various T_2 values. The flexibility and dynamics of the molecule influence the spin relaxation process; the molecules with higher mobility show higher T_2 values and vice versa. The changes in the molecules flexibility can be thus assessed by NMR spin relaxation methods.

2.3 UV-Vis spectroscopy

Ultraviolet-visible spectroscopy (UV-Vis) is an absorption spectroscopy method operating in the ultraviolet and full visible spectral regions. An electron is excited to the upper electron state at the absorption. The proper wavelength of the excitation light that corresponds to the transition energy is required. Absorbance A of a substance in a visible region is related to the colour, so we can partly predict the spectrum shape. The absorbance is counted from the Lambert-Beer law

$$A = log\frac{I_0}{I} = \varepsilon cL. \tag{2.15}$$

The intensity I_0 belongs to the excitation light and I is the intensity of the sample transmitted light. The fraction I/I_0 is called a transmitance. The absorbance of a sample is depended on concentration c, length of the absorption layer L and molar absorption coefficient ε (at a certain wave length). UV-Vis spectroscopy is often used for the concentration determination.

3. Goals of the thesis

In this thesis, the temperature-sensitive hydrogels are prepared and studied with different experimental techniques:

The particular goals of the thesis are:

- to prepare poly(N, N'-diethylacrylamide) (PDEAAm) SN hydrogels with various cross-linking density
- to prepare two series of DN hydrogels using the SN hydrogels, one with poly(acrylamide) (PAAm) and the second one with poly(N, N'-dimethylacrylamide) (PDMAAm) as the second network
- swelling experiments to study swelling and deswelling character of the samples, the collapse parameters (onset temperature, temperature interval, enthalpy, entropy) determination
- NMR spectroscopy temperature measurements for a microscopic investigation of the collapse, the collapse parameters determination
- NMR relaxation experiments using CPMG sequence to determine spin-spin relaxation time, the characterisation of water molecules dynamics in the sample
- UV-Vis spectroscopy for studying a model molecule release out of the swollen hydrogel structure, a qualitative description of the release

4. Preparation

4.1 Single networks

The first of all, we prepared the SN hydrogels, which are needed for a DN synthesis, but they are also studied as a separate series.

The single network (SN) hydrogels were prepared by a redox polymerization of aqueous solutions containing monomer, N, N'-diethylacrylamide (DEAAm), figure 4.1, and cross-linking agent, N, N'-methylenebisacrylamide (MBAAm), figure 4.2. Depending on MBAAm amount, the networks is more or less cross-linked.

The first sample was made from 0.36 g of DEAAm and 0.01 g of MBAAm mixed at 5 °C in 5 ml of N_2 saturated H_2O. Then 250 μL of 2 % AMPS/H_2O and 75 μL of TEMED were added. The solution was injected into the forms with $\sim$2 mm of depth and kept at 5 °C. The gelation process is very fast and happens in a couple of minutes. After half an hour, the gel was situated in distilled water to clear for 1 h and 12 hrs.

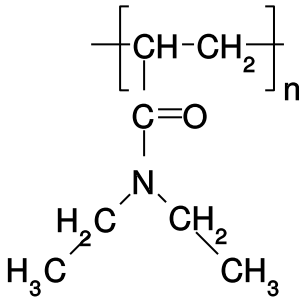

Figure 4.1: Poly(N, N'-diethylacrylamide) (PDEAAm)

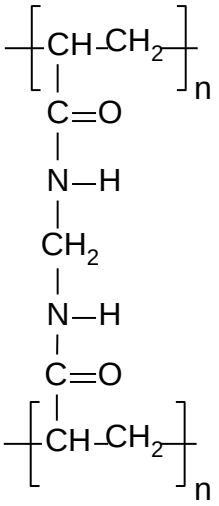

Figure 4.2: Polymerized MBAAm

Other samples were prepared the same way but with different amount of MBAAm, see table 4.1, the numbers stand for a label of the sample with certain cross-linking density.

	1	2	3	4	5	6
MBAAm/g	0.010	0.008	0.006	0.004	0.002	0.001

Table 4.1: Mass of MBAAm in the samples

4.2 Double networks

A preparation process of the double networks is shown in figure 4.3. The single network hydrogel is swollen in the monomer solution of the second component, it is cross-linked with UV radiation later. Chains of the both networks entwine each other.

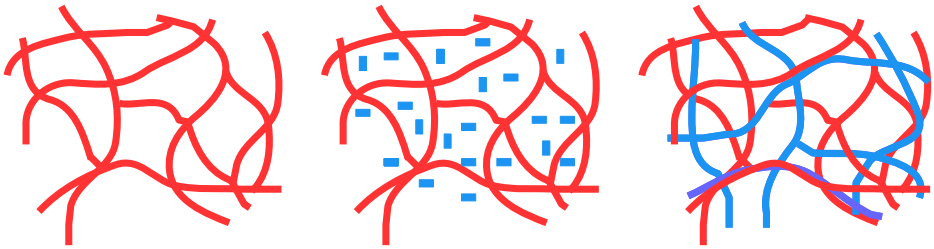

Figure 4.3: Model of double network formation

The preparation of the DN hydrogels demands solutions of AAm 4.4 and DMAAm 4.5. AAm solution was prepared in 700 mL of distilled water mixing 99.51 g AAm, 0.108 g MBAAm, 0.102 g OGA. DMAAm solution was prepared in 700 mL of distilled water mixing 138.8 g DMAAm, 0.108 g MBAAm, 0.102 g OGA.

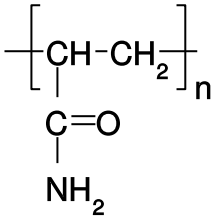

Figure 4.4: Poly(acrylamide) (PAAm)

The samples of PDEAAm (SN) were cut and one piece was left to swell in AAm and the second one in DMAAm solution. These samples were radiated with UV lamp for 3 hours, which made the polymerization of the second network and double network was formed.

After the preparation, there were three series of samples, table 4.1: the SN series, the DN series with PAAm as the second network and DN series with DMAAm as the second network, each of them containing six samples of different first network densities. In sum, eighteen samples were prepared.

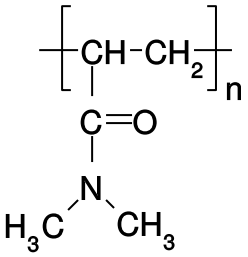

Figure 4.5: Poly(N, N'-dimethylacrylamide) (PDMAAm)

SN	**DN PAAm**	**DN PDMAAm**
PDEAAm 1	PDEAAm/PAAm 1	PDEAAm/PDMAAm 1
PDEAAm 2	PDEAAm/PAAm 2	PDEAAm/PDMAAm 2
PDEAAm 3	PDEAAm/PAAm 3	PDEAAm/PDMAAm 3
PDEAAm 4	PDEAAm/PAAm 4	PDEAAm/PDMAAm 5
PDEAAm 5	PDEAAm/PAAm 5	PDEAAm/PDMAAm 5
PDEAAm 6	PDEAAm/PAAm 6	PDEAAm/PDMAAm 6

Table 4.2: Prepared samples

5. Measurement and results

Although six different cross-linking densities of PDEAAm were prepared, only three (marked 1, 3 and 5 in table 4.2) of each series were examined properly and the results are summarized in this chapter.

All of eighteen samples were measured in swelling experiments, but we found out that their behaviour is well proportional to the cross-linking density, therefore using only three samples of each series were sufficient to characterize them clearly.

5.1 Swelling experiments

First of all, we took a small piece of each sample and weighed it, left it to dry out for a couple of days and weighed it again. This is how we get the mass of hydrogel at the room temperature $m(298\ \mathrm{K})$ and the mass of the polymer network m_{dry} after drying the hydrogel out. These quantities helped us to get the mass fraction of polymer network at the room temperature 5.1,

$$w_p(298\ K) = \frac{m_{dry}}{m(298\ K)} \tag{5.1}$$

which is used to obtain temperature depending polymer mass fraction w_p according to expression 5.2.

$$w_p(T) = w_p(298\ K)\frac{m'(298\ K)}{m(T)} \tag{5.2}$$

In this expression, $m'(298\ \mathrm{K})$ is the mass of sample used for swelling experiments at 298 K and $m(T)$ is the mass of sample at temperature T.

Fitting the dependency, the enthalpy ΔH, entropy ΔS and characteristic temperature of the transition can be reached. The swelling and deswelling may be considered as a change between the bound water m_{bound} and free water m_{free} in the swollen or collapsed hydrogel. The process is controlled by the Gibbs free energy and described by a temperature change of the equilibrium constant K.

$$lnK = -\frac{\Delta H}{RT} + \frac{\Delta S}{R}, \tag{5.3}$$

where ΔH and ΔS stand for the enthalpy and entropy change and R is the gas constant. At the same time, the equilibrium constant K can be expressed as the ratio of the bound and free water

$$K = \frac{m_{free}}{m_{bound}}. \tag{5.4}$$

The total mass of water in a sample at 298 K equals

$$m_0 = m_{PB} + m_{free} + m_{bound}, \tag{5.5}$$

where m_{PB} is permanently bound water. The hydrogel mass at temperature T is equal to

$$m'(T) = m_{dry} + m_{PB} + m_{bound} \tag{5.6}$$

and then the constant K can be expressed as

$$K = \frac{m'(298K) - m'(T)}{m'(T) - m_{dry} - m_{PB}} \tag{5.7}$$

Using equations 5.4 - 5.7, the final formula for mass fraction of polymer network w_p at temperature T is

$$w_p(T) = \frac{1 + K}{\frac{m'(T_0)}{m_{dry}} + (1 + \frac{m_{PB}}{m_{dry}})K} \tag{5.8}$$

The samples were situated into the phials, figure 5.1, heated and weighed with step 1 K every 30 minutes.

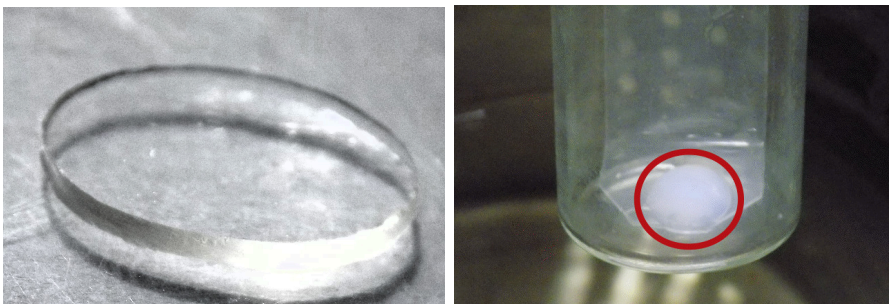

Figure 5.1: Hydrogel before (left) and after (right) heating in the phial

5.1.1 Extent of swelling

The mass polymer ratio is a quantity showing the rate of the swelling, how much the sample tend to swell. The initial mass polymer ratio for the samples is in table 5.1.

	SN	***DN/PAAm***	***DN/PDMAAm***
1	0.11	0.16	0.06
3	0.08	0.12	0.05
5	0.04	0.08	0.03

Table 5.1: Intial mass fraction of polymer

The smaller mass polymer fraction is, the more water is contained in the sample. So in the column of the SN results, the most water was swollen in sample 5, which is the sample with the smallest network density. Thus, the network density affects the amount of the swollen water inversely. This trend is the same in the columns for the DN. The different cross-linking density creates a network with the different average length of polymer chains between two network junctions that makes them less or more accessible for the water molecules, figure 5.2.

If we compare the SN and DN, we generally cannot tell whether the second network makes the sample more or less hydrophilic, it is dependent on the character of the second network. In our case, the DN with PDMAAm tend to swell more than the SN, but the DN with PAAm tend to swell less.

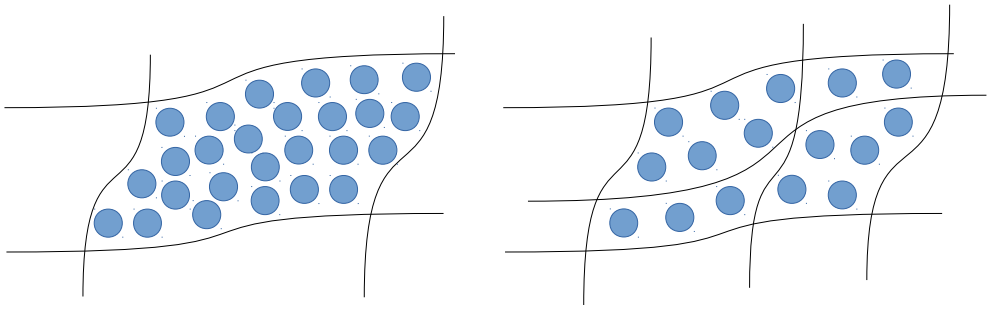

Figure 5.2: Water molecules in networks of different cross-linking density

5.1.2 Parameters of collapse

The measured temperature polymer mass dependencies are shown in the figures 5.3, 5.4 and 5.5. All of them were fitted with 5.8.

At first sight, the collapse is the most significant in the SN series, it is the fastest and reports the greatest polymer mass fraction change, the greatest water loss. It is caused by the absence of the second, temperature-insensitive and hydrophilic component, which decreases the extent and increases the temperature onset and interval of the collapse.

	ΔH	ΔS	m_{PB}	T_{on}	ΔT
	kJ.mol^{-1}	J.mol^{-1}.K^{-1}	mg	K	K
PDEAAm 1	246	832	31	290	12
PDEAAm 3	284	954	34	292	10
PDEAAm 5	289	971	24	293	10
PDEAAm/PAAm 1	211	694	84	297	15
PDEAAm/PAAm 3	199	652	110	297	16
PDEAAm/PAAm 5	152	505	165	292	20
PDEAAm/PDMAAm 1	141	460	127	295	22
PDEAAm/PDMAAm 3	115	374	125	293	27
PDEAAm/PDMAAm 5	90	295	198	288	34

Table 5.2: Fitting parameters of w_p temperature dependency

The fitting parameters from equation 5.8 for all studied hydrogels are summarized in table 5.2.

The SN entropy and enthalpy slightly differ but do not report any obvious trend in the dependency of collapse on the network density. On the other hand, the entropies and enthalpies for double networks PDEAAm/PAAM and PDEAAm/PDMAAm decrease with the descending network density. So the possible interpretation is that that the DN hydrogels with lower crosslinking density show generally less intensive collapse. This explanation is not working for the SN though.

The most likely explanation is related to the process of the preparation, during which the final proportion of PDEAAm and PAAm changes for different network densities. The samples of PDEAAm with higher network density probably swell less amount of monomers AAm or DMEAAm during the polymerization of the second component than those with lower network density. That leads to the dis-

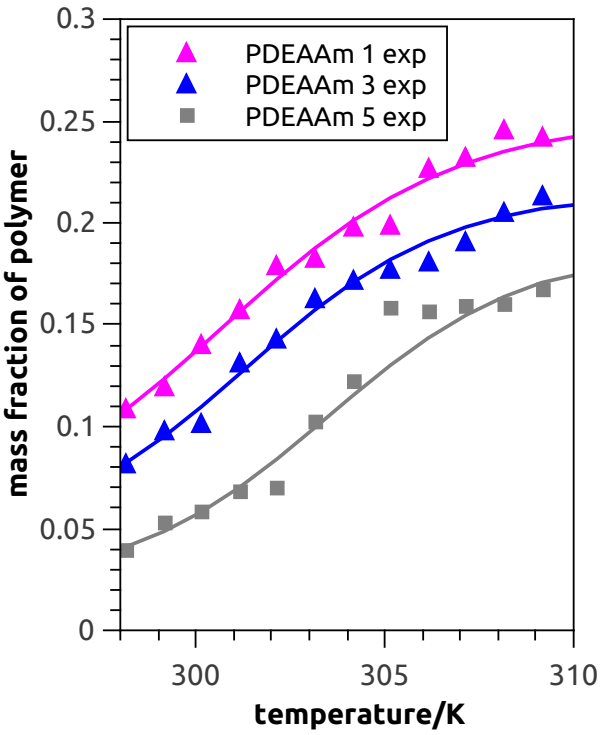

Figure 5.3: Polymer fraction mass temperature dependency for SN hydrogels

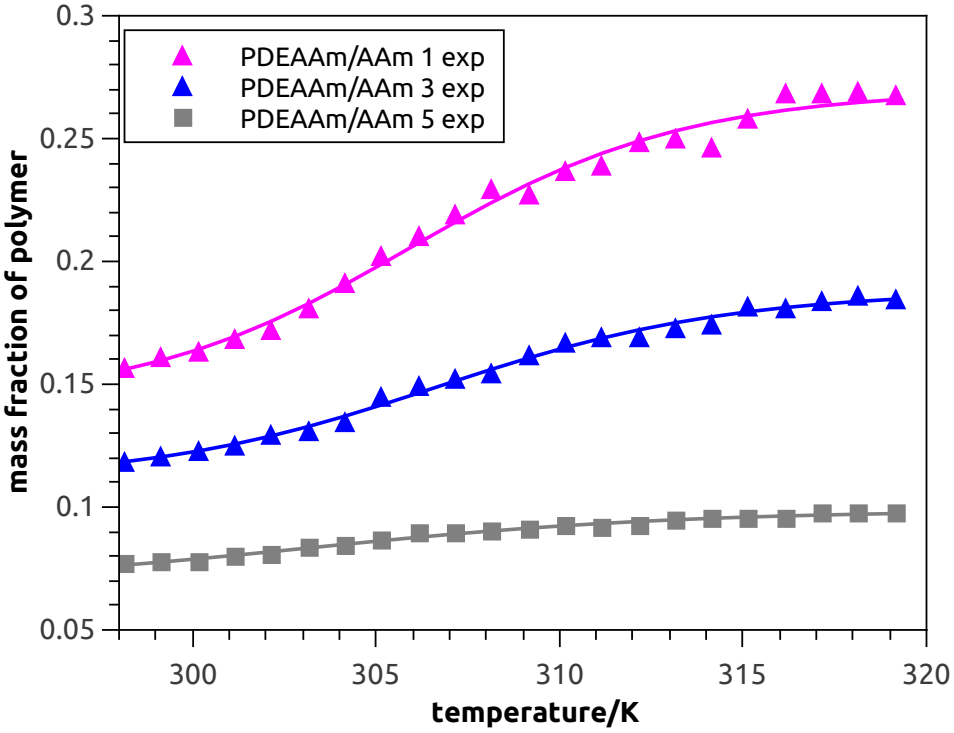

Figure 5.4: Polymer fraction mass temperature dependency for DN/AAm hydrogels

cussed dependency between the extent of the collapse described with entropy and enthalpy and the network density, as the more temperature insensitive component is contained, the less intensive collapse happens (because the quantities are

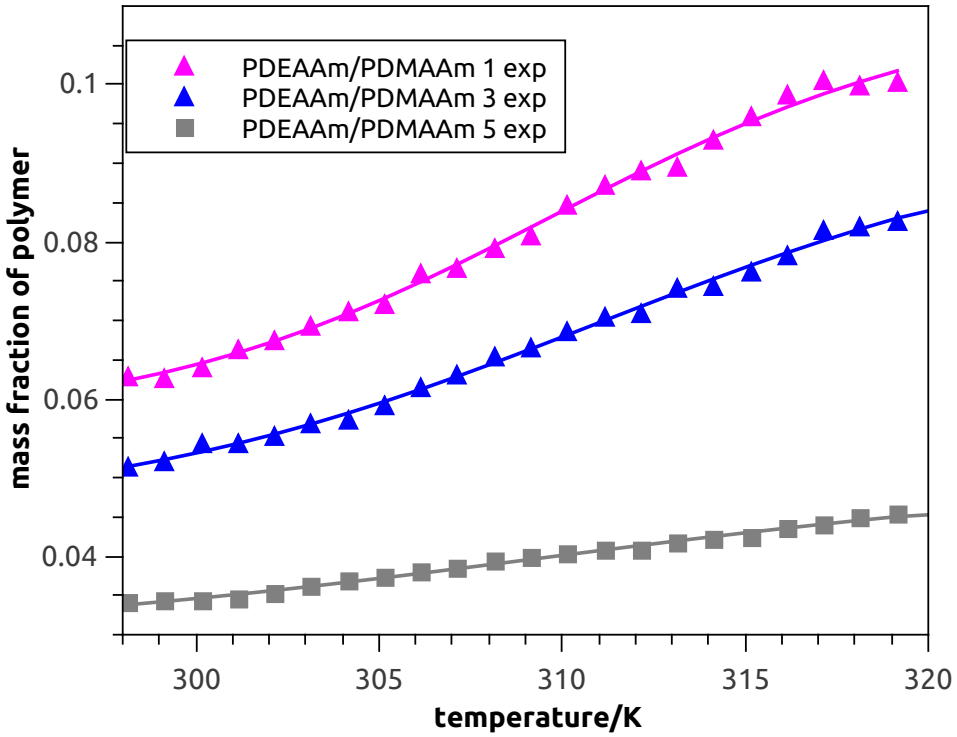

Figure 5.5: Polymer fraction mass temperature dependency for DN/DMAAm hydrogels

related to the total mass of the sample).

It is obvious that double networks have smaller enthalpy and entropy of the collapse. It is caused by the fact that these quantities are related to the amount of the component and double networks contain both temperature sensitive and non-sensitive part as well, in contrast with single network containing only the temperature sensitive substance.

The presence of the second part also influences the temperature interval of the collapse. The first network component (PDEAAm) is less sensitive to temperature due to the presence of the second hydrophilic network and needs a higher temperature to prevail over it and change its conformation. Temperature intervals differ for the different cross-linking densities of the DN, because the less cross-linked samples contain larger amount of hydrophilic, temperature non-sensitive component, which limits the collapse of sensitive PDEAAm.

The DN hydrogels contain much more permanently bound water above the transition, because they include temperature non-sensitive, hydrophilic part binding water even at higher temperatures.

5.2 NMR spectra

Figure 5.6: Sample NMR

Nuclear magnetic resonance spectroscopy was used to examine the hydrogel collapse microscopically. NMR sample were prepared from a piece of the swollen hydrogel and deuterated water 5.6. Less flexible structures are not visible in the NMR spectrum, wide spectral bands belong to less flexible molecules, so they are not visible because of the width in a spectrum of a high resolution. The originally flexible molecules conformationally changes during the collapse and the narrow peaks become wider and smaller so in the result they are not noticeable.

It is necessary to mention that this effect concerns only the temperature-sensitive constituent so there are also signals in 5.7 from PAAm (resp. PDMAAm) that stay unchanged.

Measuring spectra with growing temperature from 298 K to 330 K with step 0.5 K, we get set of spectra, whose section is shown in 5.7.

The first spectrum of the measured series is chosen and its parameters (the intensity of each peak I_0 and temperature T_0) are used to calculate the quantity called p-factor. It describes the fraction of the collapsed polymer units, which were originally seen in the NMR spectra.

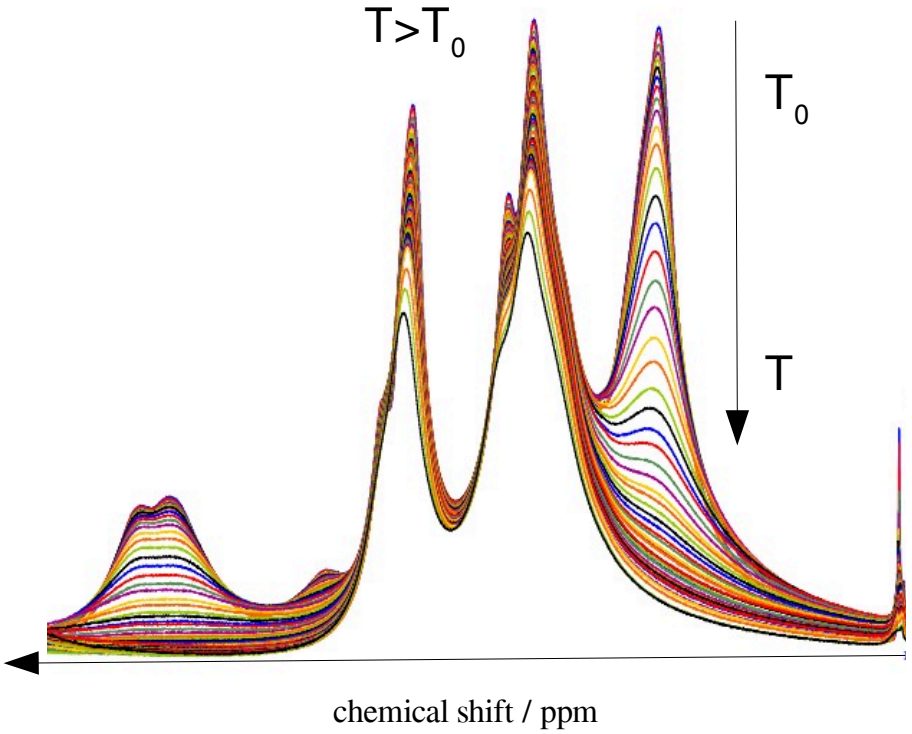

Figure 5.7: A section of NMR spectra PDEAAm/PAAm, measured with growing temperature

p-factor [23] is calculated according to

$$p = 1 - \frac{I}{I_0}\frac{T}{T_0}, \tag{5.9}$$

where I is the intensity of a certain peak at temperature T. It is obvious that p-factor is a temperature dependent quantity, the higher temperature, the bigger fraction of the collapsed units. p-factor temperature dependency could be deduced also theoretically. We supposed the equilibrium constant for the collapsed and free units

$$K = \frac{p}{p_{max} - p}, \tag{5.10}$$

where p_{max} is the maximal value of p-factor. This constant also can be expressed using Gibbs free energy ΔG as

$$K = e^{\frac{\Delta G}{RT}}. \tag{5.11}$$

Finally, p-factor is derived as

$$p = \frac{p_{max}}{1 + e^{\frac{\Delta H}{RT} - \frac{\Delta S}{R}}}. \tag{5.12}$$

5.2.1 Measured spectra

The measured spectrum of the SN at 298 K is in figure 5.8. Each of measured spectra contains the peak of water, which is about 4.8 ppm, and the peak of standard at 0 ppm, which is inert and serves as a calibration to compare the peak chemical shifts. The rest of the signals correspond to the hydrogen protons from PDEAAm 4.1. Peak about 1.2 ppm belongs to the methyl groups of the ethylene in the side chain. CH_2 group of ethylene has signal at 3.6 ppm and the last two signals (2.6 and 1.7 ppm) are proton signal of PDEAAm backbone.

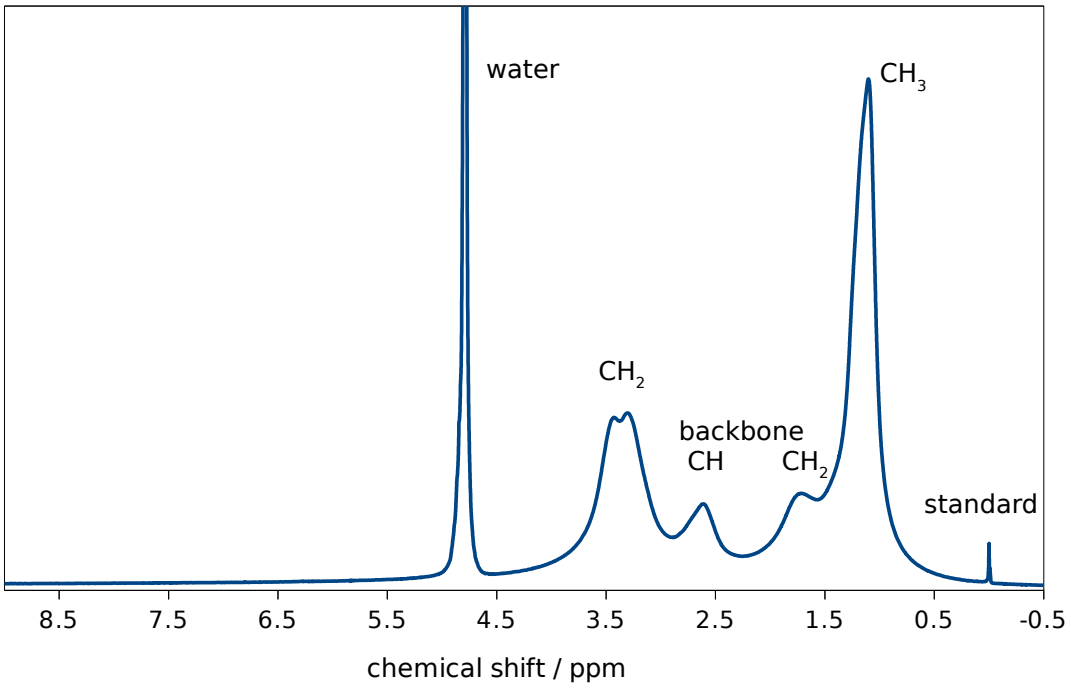

Figure 5.8: NMR spectrum of PDEAAm at 298 K

In figure 5.9, there is a spectrum of the DN PDEAAm/PAAm to compare. The structures of both networks are shown in 4.4 and 4.1. There are a couple of

differences between figures 5.8 and 5.9. The new signals at 7 ppm and 7.7 ppm appear belonging to NH_2 group of PAAm. It is also obvious that the signal of the backbone is much greater than in figure 5.8, which is except for the contribution of PDEAAm caused also the contribution of the backbone of PAAm.

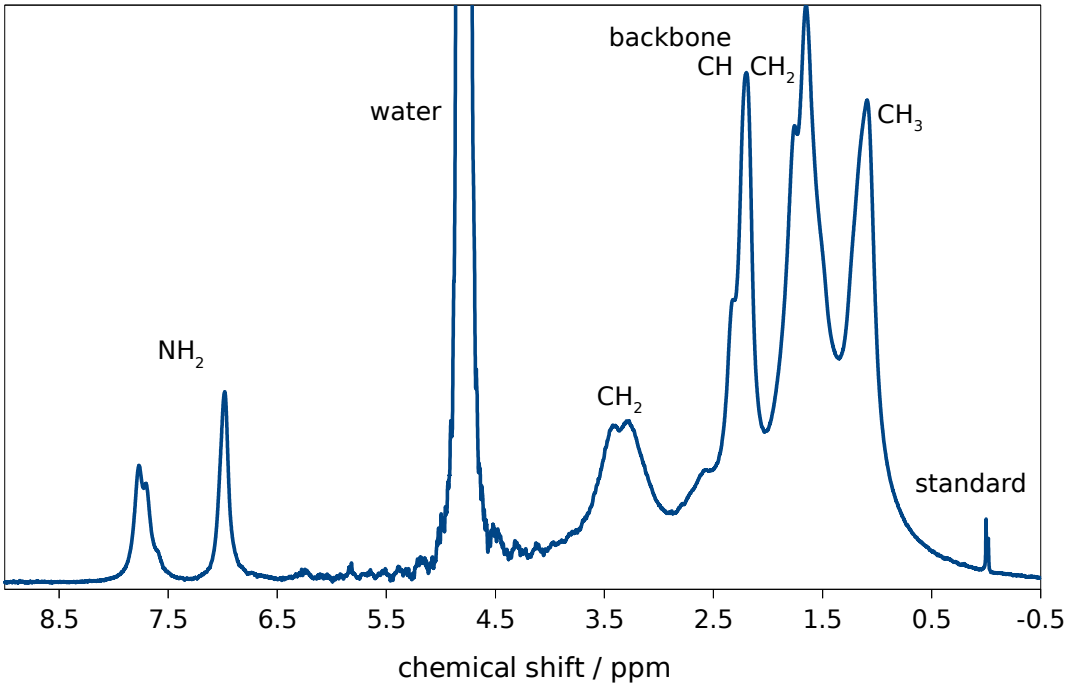

Figure 5.9: NMR spectrum of PDEAAm/PAAm at 298 K

Spectra of the DN with PDEAAm/PDMAAm (structure in 4.1 and 4.5) are then well predictable. The peaks of NH_2 are not there, and if we compare the structures of PDEAAm and PDMAAm, it is obvious that apart from CH_2 of ethylene every peak will be a contribution of PDEAAm as well as PDMAAm.

The spectra measured above the critical temperature (at 327 K) are shown in figures 5.10 for PDEAAm and 5.11 for PDEAAm/PAAm. PDEAAm hydrogel is temperature-sensitive so there will be only the water signal in the spectrum after the collapse. PDEAAm/PAAm contains temperature-sensitive PDEAAm as well as temperature-nonsensitive PAAm, whose signal remains in the spectrum together with the water signal after the collapse.

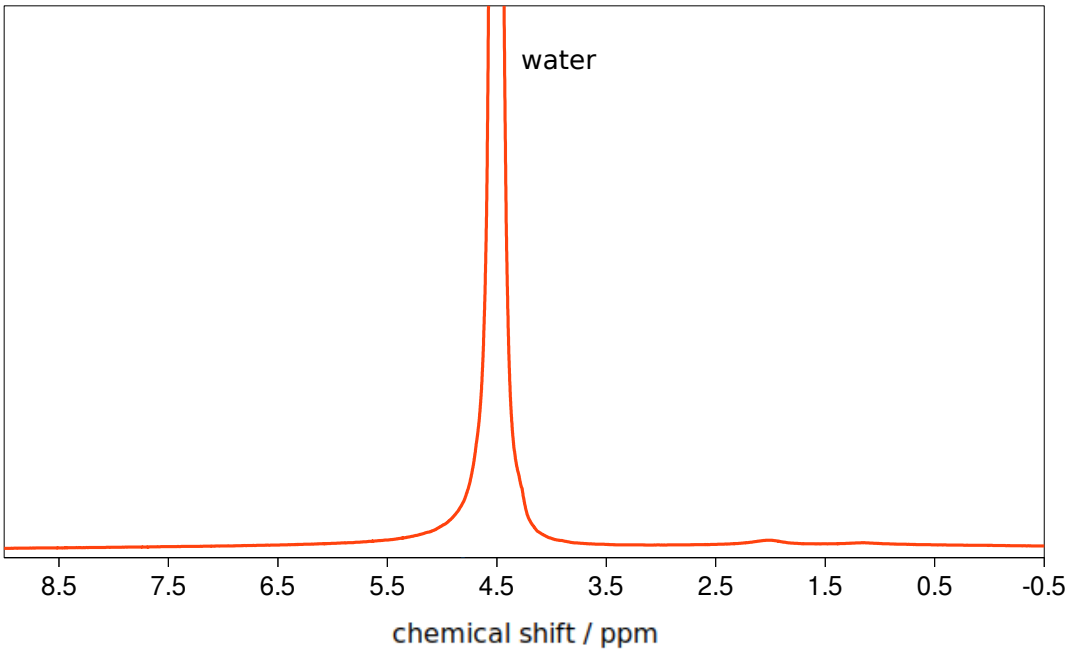

Figure 5.10: NMR spectrum of PDEAAm at 327 K

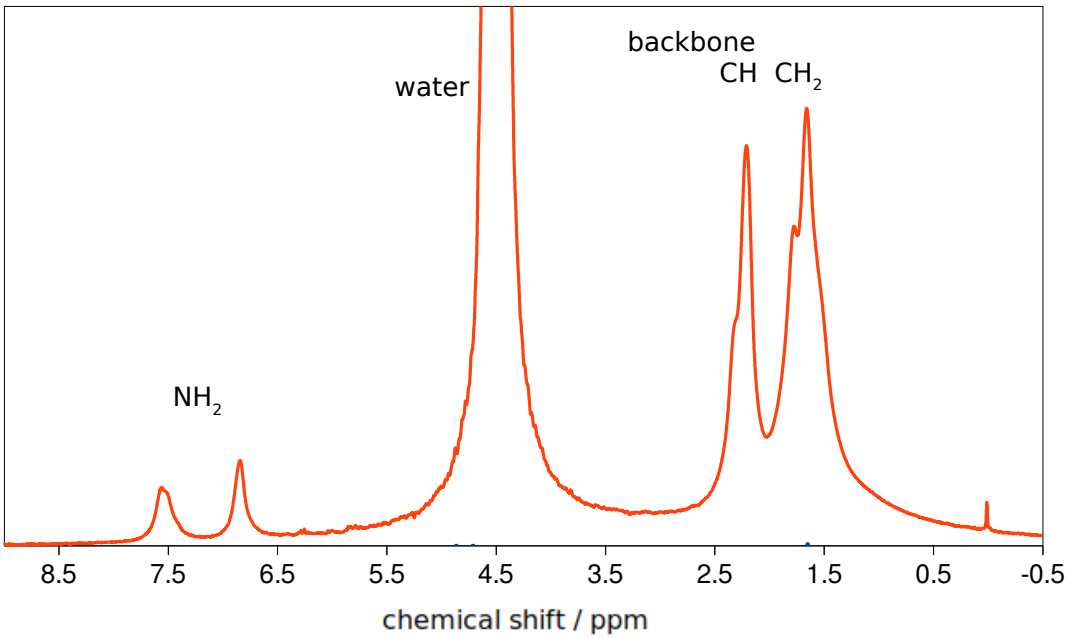

Figure 5.11: NMR spectrum of PDEAAm/PAAm at 327 K

5.2.2 Temperature dependency

Spectra with the growing temperature were measured for all samples. It was obtained a set of the spectra shown in 5.7 for every sample. Formulas 5.9 and 5.12 were used to get the final results, which are shown in figure 5.12 and summarized in table 5.3.

In the p-factor temperature dependency, the entropy and enthalpy of the collapse are represented by the slope of the curve. The greater slope, the bigger measured quantities. In figure 5.12 and also in table 5.3,the entropy and enthalpy

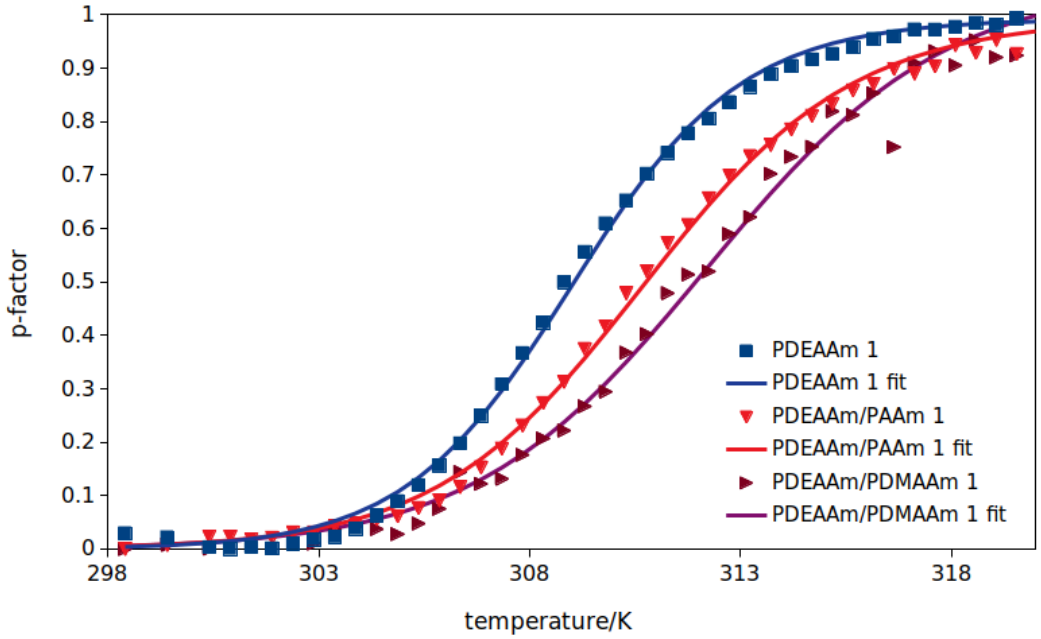

Figure 5.12: p-factor temperature dependency for the highest cross-linking density (1) of SN, DN with PAAm and PDMAAm

prove that the greatest collapse range is reported in the case of SN, smaller is for the DN with PAAm and the smallest for the DN with PDMAAm.

Any obvious trend is not presented comparing the various cross-linking densities of a certain series. The differences are tiny and can be caused by the measurement error.

Temperatures of the beginning of the collapse T_{on} are generally higher for the DN hydrogels, the highest for the DN with PDMAAm. All these values although differ very slightly and contain deviations that might be caused by the measurement and the fitting accuracy.

The temperature interval of the collapse is the shortest in case of the SN. The DN hydrogels contain temperature-insensitive hydrophilic component, which restricts the sensitive one and prolongs the temperature interval. ΔT is greater for the DN with PDMAAm because PDMAAm is generally more hydrophilic than PAAm, see table 5.1.

	ΔH	ΔS	T_{on}	ΔT
	kJ.mol^{-1}	J.mol^{-1}.K^{-1}	K	K
PDEAAm 1	398	1289	305	8
PDEAAm 3	422	1374	303	7
PDEAAm 5	387	1251	306	8
PDEAAm/PAAm 1	324	1043	306	10
PDEAAm/PAAm 3	320	1028	306	10
PDEAAm/PAAm 5	333	1078	305	10
PDEAAm/PDMAAm 1	289	926	307	11
PDEAAm/PDMAAm 3	276	884	307	12
PDEAAm/PDMAAm 5	245	786	305	13

Table 5.3: Fitting parameters of p-factor temperature dependency

5.3 NMR relaxation experiments

Water is bound in the hydrogel samples in different ways. Some molecules are more or less flexible than the others due to that [24]. The flexibility of water can be measured with relaxation experiments on NMR spectrometer, respectively the relaxation of HDO molecules. The spin-spin relaxation time T_2 is investigated with CPMG sequence in figure 2.4.

Hydrogel samples were prepared the same way as for measuring the spectra 5.6. At first, the relaxations were set for a sample at 290 K. Then heating started and the next relaxations were measured at 318.5 K. The system was reaching the equilibrium at 318.5 K and then measuring started after 24 hours again at 318.5 K.

The time dependency of HDO signal during the relaxation process was obtained, see figure 5.13. We need to set the experiment parameters properly to get enough data points. The data points have to well characterize the important parts of the curve to provide better accuracy of fitting.

We tried a couple of combinations for the parameters values and the best results were reached with: $NS = 8, DS = 2, D1 = 100$ s, $D20 = 0.5$ s.

We presumed there could be a kind of the free and bound water in the sample. It corresponds with fitting the dependency. It is necessary to use the double exponential decay because the monoexponential one does not follow the data points very precisely. Thus, the dependencies of all samples were fitted with the expression:

$$I(t) = a^1 e^{-T_2^1} + a^2 e^{-T_2^2}, \tag{5.13}$$

where I stands for measured intensity, t for time, $a^{1,2}$ for pre-exponential factors and $T_2^{1,2}$.

The results are summarized in 5.4. If a contribution of T_2^1 or T_2^2 was bigger than 5% (one of the pre-exponential coefficients $a^{1,2}$ outreaches value 0.05), it is written in the table, otherwise it is neglected. Pre-exponential factors $a^{1,2}$ are given in the brackets if there were both $T_2^{1,2}$ significant.

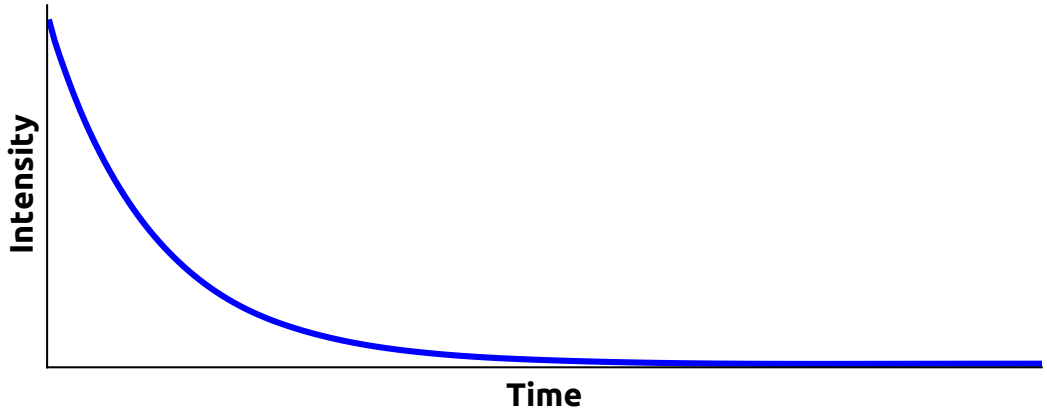

Figure 5.13: Time dependency of signal intensity

If we look in table 5.4, we can see that the water in DN PDEAAm/PDMAAm hydrogels has only one T_2 in a couple of seconds belonging mainly to the free water. The free water relaxation time is longer than for the bound water. PDEAAm/PDMAAm is a hydrogel with a high swelling ratio. The polymer network is surrounded by a large amount of molecules which are very weakly bound and behave rather like free water.

The water in the SN hydrogels seems to be free at 290 K. The bound water (with much shorter T_2) is noticeable after heating to 318.5 K and tend to disappear after 24 hours at 318.5 K. The bound water is in the collapsed structure more tighten but tend to release when reaching the equilibrium. This theory is not consistent with sample PDEAAm 3, pre-exponential factor is a bit bigger after 24 hours, but it could be the error of the fit or measurement.

The bound water from the SN hydrogels was not observed in the DN with PAAm. The relaxation time around 1 s appears after the collapse. This value is too high to belong to the bound water but may be caused by an effect of water molecule diffusion from the more hydrophilic part to the collapsed structures. The collapsed structures of the DN are not so tighten as in the SN, because of the limiting by the hydrophilic, temperature-nonsensitive part. The water (with $T_2 \sim 1s$) seems to diffuse from an open to more closed space, which could be represented heterogeneous, maybe porous structure of the DN with PAAm hydrogel network.

	T_2^1	T_2^2
	s	s
PDEAAm 1		
290 K		3
318.5 K	0.1 (0.12)	2.2 (0.88)
318.5 K 24 h	0.1 (0.08)	2.5 (0.92)
PDEAAm 3		
290 K		4.4
318.5 K	0.03 (0.07)	4.8 (0.93)
318.5 K 24 h	0.001 (0.11)	6.6 (0.89)
PDEAAm 5		
290 K		4.1
318.5 K	0.04 (0.11)	5.1 (0.89)
318.5 K 24 h		5.5
PDEAAm/PAAm 1		
290 K		4.3
318.5 K	1.2 (0.12)	4.0 (0.88)
318.5 K 24 h	1.4 (0.17)	4.5 (0.83)
PDEAAm/PAAm 3		
290 K		3.9
318.5 K		3.3
318.5 K 24 h	1.1 (0.12)	4.2 (0.88)
PDEAAm/PAAm 5		
290 K		3.0
318.5 K	0.001 (0.13)	2.6 (0.87)
318.5 K 24 h	1.6 (0.28)	3.4 (0.72)
PDEAAm/PDMAAm 1		
290 K		3.8
318.5 K		4.1
318.5 K 24 h		4.0
PDEAAm/PDMAAm 3		
290 K		3.1
318.5 K		3.8
318.5 K 24 h		4.0
PDEAAm/PDMAAm 5		
290 K		3.7
318.5 K		4.3
318.5 K 24 h		4.5

Table 5.4: Spin-spin relaxation times of water in samples

5.4 UV-Vis spectroscopy

UV-Vis spectroscopy is one possibility how to investigate the solvent releasing from a hydrogel during the collapse. Using a model solvent absorbing in the range of UV-Vis spectrometer is needed then. Hence, methylene blue was chosen as if it was successfully used in [25]. The chemical structure of methylene blue (MB) is shown in figure 5.14.

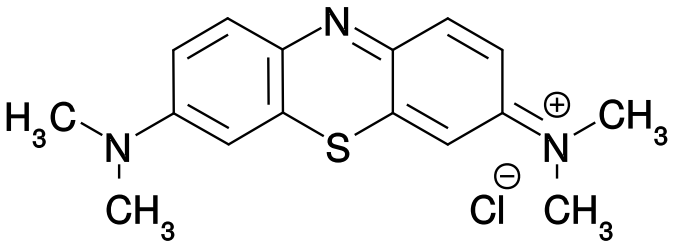

Figure 5.14: Chemical structure of MB

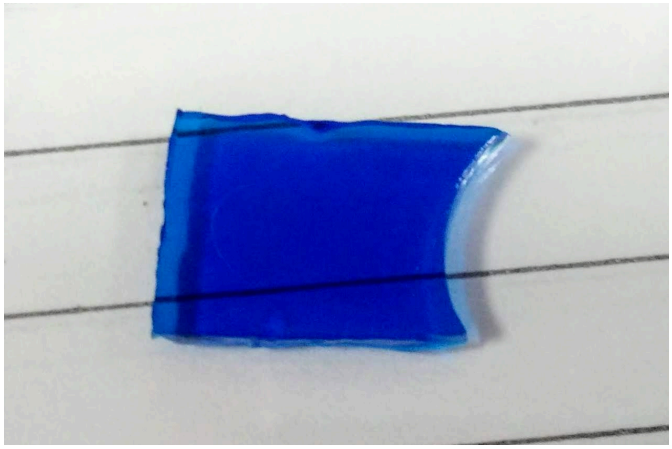

Figure 5.15: Hydrogel swollen in MB solution

At first, it was necessary to determine the concentration of the model solution in which the samples would be swollen. The final solution (surrounding deswolllen hydrogel) must be measurable with UV-Vis spectrometer, it means that measured intensity of an absorption is not allowed to overstep a certain value to protect that logarithmic relation between optical density and concentration (see equation 2.15) is preserved.

After a few tests, we finally prepared MB solution:

1 portion of MB solution with concentration (1.5 g MB/100 ml H_2O)
+
10 portion of H_2O

The experiment itself consists of several steps:

1. cutting a piece of hydrogel off ($\sim$ 2 cm^2), weighing
2. drying at room temperature for 3 days, weighing
3. swelling in MB solution (5 ml) for a couple of days, figure 5.15
4. weighing, preparation of water bath (318.5 K), heating phials filled with 4 ml of water
5. adding the swollen hydrogel in MB solution
6. measuring an absorption of the solution surrounding the sample in time

The collapsed samples of SN hydrogels are shown in figures 5.16 and 5.17.

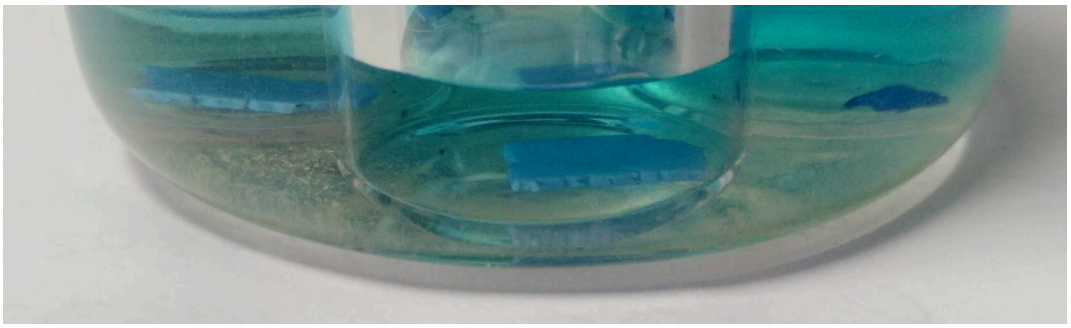

Figure 5.16: Collapsed SN hydrogels originally swollen in MB solution (from left PDEAAm 1, PDEAAm 3, PDEAAm 5)

Figure 5.17: Collapsed PDEAAm 1 originally swollen in MB solution

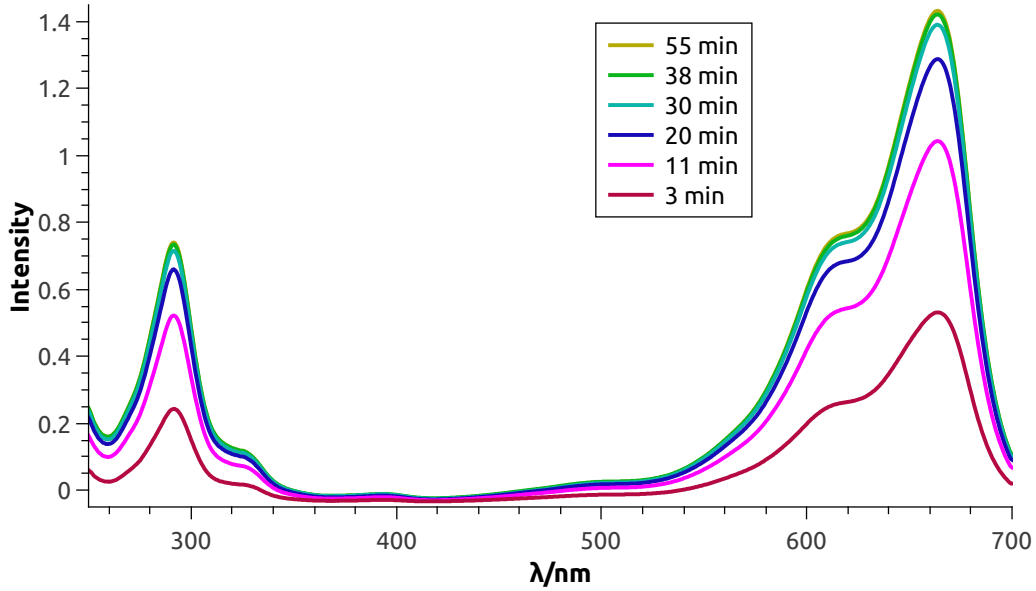

Figure 5.18: UV-Vis spectra of MB measured after various time periods from immersion the hydrogel DN PDMAAm 1 in the phial

An absorption spectrum of MB is in figure 5.18. The signal of maximum intensity at 664 nm served to compare the individual spectra. In figure 5.18, there are spectra of measured PDEAAm/PDMAAm 1 for example. The solution in the phial was taken 3, 11, 20, 30, 38 and 55 minutes after immersion the MB swollen hydrogel into pure water at 318.5 K. During the time, more and more MB molecules is released out of the hydrogel and the concentration of MB in the outer solution surrounding the sample gets higher. The higher concentration of MB, the more radiation is absorbed. Hence, the spectral bands are more intensive with time as shown in figure 5.18.

The intensity of the signal at 664 nm was used for the MB concentration determination. The time dependency of MB concentration can be drawn then, see figures 5.19, 5.20, 5.21.

Each of these dependencies was fitted with expression

$$c(t) = c_{max} - b\exp(-t/\tau), \tag{5.14}$$

where $c(t)$ is the concentration of MB in the solution surrounding the hydrogel sample, c_{max} is the maximum concentration of the surrounding solution, b is a coefficient and τ stands for time which is taken to reach the equilibrium.

The parameters of fitting are summarized in table 5.5.

In the figures 5.19, 5.20, 5.21, we can see that the dependency 5.14 describes the measured data very well for all samples apart from sample PDEAAm 5. This sample has the lowest cross-linking density and it is obvious that collapse happens very quickly and that almost all MB is released immediately. The samples with higher cross-linking densities of the SN hydrogels do not show this behaviour. Another interesting feature in PDEAAm 5 dependency is the lowering MB concentration for longer period. MB might bond back with the polymer collapsed network and tend to stack. Different behaviour of PDEAAm 5 is visible in figure 5.16, its volume in collapsed state is much smaller than other SN samples

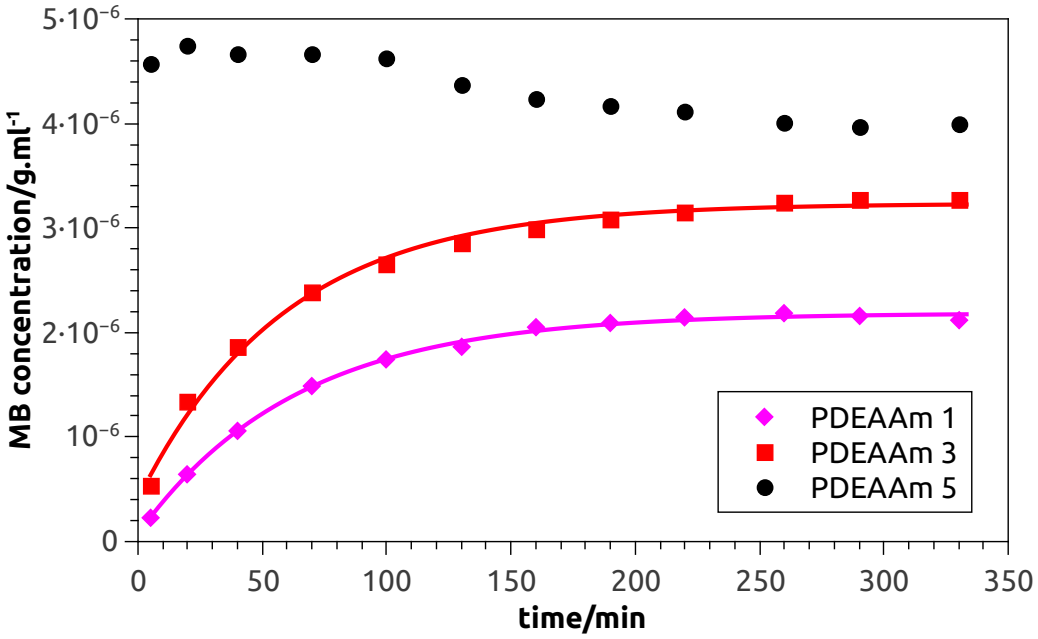

Figure 5.19: Time dependency of MB concentration for releasing process from SN hydrogels

although the swollen samples were approximately of the same size.

The maximum concentrations c_{max}, the plateaus of the dependencies cannot be compared among several samples because the exact amount MB swollen in the sample is unknown (a different size of samples and different polarity, swelling and chemical properties of the samples). The fraction of released MB can be calculated though if swelling properties are considered, see table 5.6. The shape of dependencies is the feature that give us information about time τ, got exactly from fitting. The values are summarized in table 5.5.

In table 5.5, the parameter describing time, which is necessary to release the maximum of MB τ, is much longer for the SN. It is caused by the range of the collapse, which is much more significant in the SN hydrogels.

The fractions of the released MB $f(MB)$ are written in table 5.6, we can see that for PDEAAm/PAAm 1 is bigger than 1 which has no sense, but it could tell us that the accuracy of these experiments is about 10% - 20%. The values for other samples are between 0.69 and 0.96 that do not really tell us an essential information, if the estimated accuracy is considered.

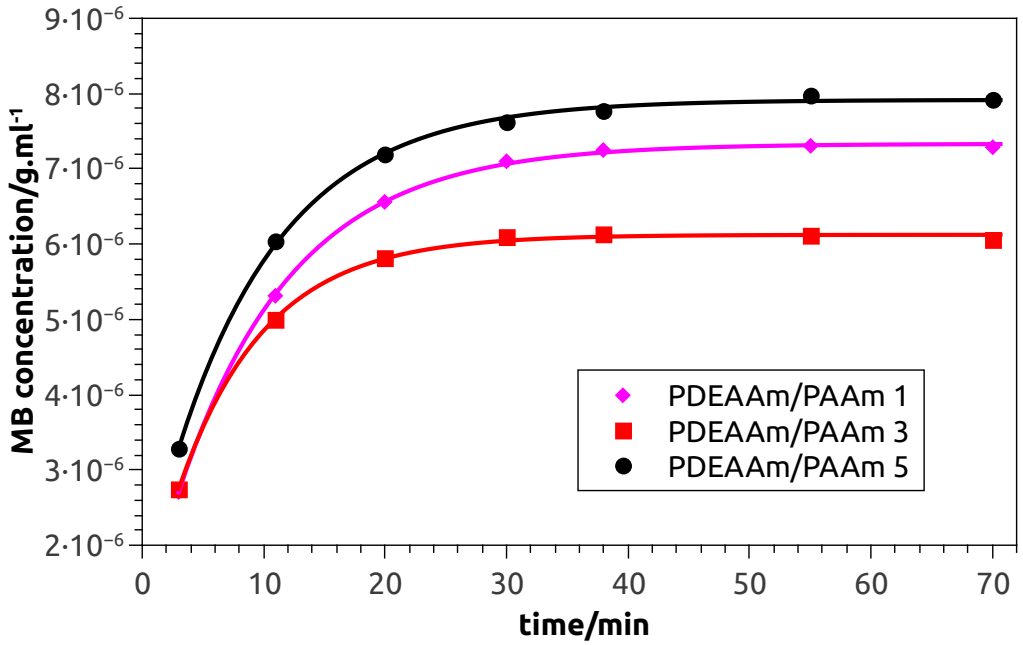

Figure 5.20: Time dependency of MB concentration for releasing process from DN PAAm hydrogels

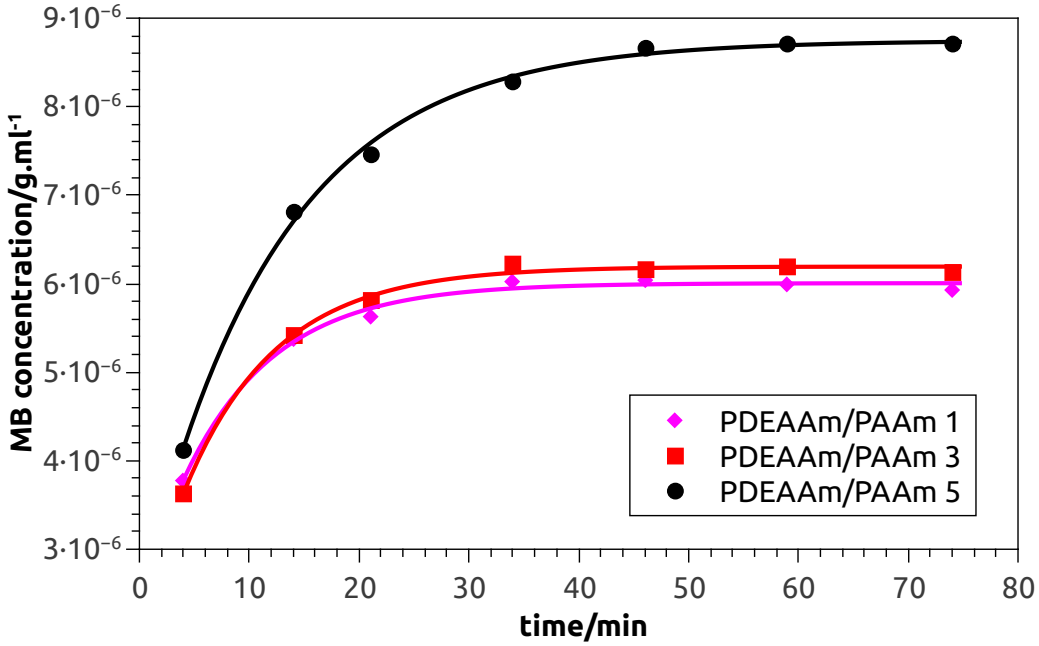

Figure 5.21: Time dependency of MB concentration for releasing process from DN PDMAAm hydrogels

	c_{max}	b	τ
	g.ml^{-1}	g.ml^{-1}	min
PDEAAm 1	2.2	2.1	64
PDEAAm 3	3.2	2.8	59
PDEAAm/PAAm 1	7.3	6.4	9.5
PDEAAm/PAAm 3	6.1	5.1	7.2
PDEAAm/PAAm 5	7.9	6.4	9.1
PDEAAm/PDMAAm 1	6.0	3.6	8.3
PDEAAm/PDMAAm 3	6.2	4.1	8.4
PDEAAm/PDMAAm 5	8.8	6.4	12.3

Table 5.5: Fitting parameters of MB concentration time dependency

	$f(MB)$
PDEAAm 1	0.73
PDEAAm 3	0.96
PDEAAm 5	0.81
PDEAAm/PAAm 1	1.05
PDEAAm/PAAm 3	0.81
PDEAAm/PAAm 5	0.89
PDEAAm/PDMAAm 1	0.69
PDEAAm/PDMAAm 3	0.71
PDEAAm/PDMAAm 5	0.76

Table 5.6: Fractions $f(MB)$ of released MB from all studied hydrogels originally MB swollen

6. Discussion

6.1 Swelling experiments

The mass polymer ratio values are contained in table 5.1. It is obvious that the values are very well adjustable with the presence and amount of the second network. The mass polymer ratio for the SN hydrogel, neat PDEAAm hydrogel can be increased or decreased with the second network of PAAm or PDEAAm, respectively. Thus, we can adjust the amount of the solution that is required. The mass polymer ratio depends on the cross-linking density proportionally, as we can see in table 5.1. Water molecules have bigger free space to fill and can better interact with hydrogen bonds in the samples with smaller cross-linking density. The same area is more separated in hydrogels with higher crosslinking density and the possible water-water interactions are disturbed by the amphiphilic character of the polymer chain. The effect is depicted in figure 5.2.

The fitting parameter corresponding to the collapse parameters are summarized in table 5.2. As long as we do not know the parameters for the SN hydrogels, we could presume that the cross-linking density impacts on the collapse proportionally. If it was true, the effect would be remarkable at the SN, but there are almost no differences for cross-linking densities 1, 3, 5 of SN. The explanation is already mentioned in the result part. The different values of the enthalpy and entropy for the DN are influenced by the composition. The amount of the monomer solution swollen during the preparation is likely set by the cross-linking density. The smaller cross-linking density, the smaller second network (swollen monomer solution) amount, the smaller enthalpy and entropy. The amount of swollen monomer solution is depended on the mass polymer ratio written in table 5.1.

The mass polymer ratio is associated with mass of permanently bound water m_{PB} in the third column of table 5.2. Although there are some inaccuracies that can be caused by a measurement error, the permanently bound water is disproportionate to the polymer mass swelling ratio at the DN that makes a good sense. At the SN, the permanently bound water is much smaller and impacted by the measurement error to find any trend of dependency.

Temperature T_{on} values do not show any reasonable dependency, the macroscopic technique swelling experiments is not probably too precise in our perform to see any trend. Though it is obvious, that the phase transition is a gradual process starting about 290 K for our samples.

The accuracy of the swelling experiments is influenced mainly by the manipulation while weighing. The (de)swollen samples are situated in water and heated. When pulling out, they are not perfectly dry on the surface. The surrounding temperature is lower than the temperature of water and collapse hydrogel changes structure and attaches some of the remaining water. This effect is very quick that even when we pull the sample and try to dry out the surface with a tissue, it is impossible to keep it unchanged, which is visible at the colour, collapsed, white clouded hydrogel gets transparent. Hence, the accuracy of the results caused by the weighing device or fitting can be negligible in comparison with the accuracy during the manipulation. The accuracy of the results from the swelling

experiments is estimated 10%.

6.2 NMR - temperature dependency

In chapter 5.2, the process of measuring hydrogels spectra at different temperatures is described. One of the most significant features while measuring polymer networks with NMR is that the polymer network is cross-linked heterogeneously. It means that some polymer chains between the junctions (see figure 1.2) are longer or shorter than the others. Due to that, just a part of the polymer chains acting like a cooperative domain is visible in spectra. The less flexible domains, usually the shorter one or those whose flexibility is limited by the second network, cannot be study in NMR spectra of high resolution. A very broad signal line belongs to the less flexible molecules that it cannot be distinguishable among the typical narrow peaks rather looks as a background.

This effect is used for measuring the spectra of collapsed structures with increasing temperature, whose flexibility is more and more limited and the intensity of the narrow lines gets smaller, because some of the domains get tight and its signal is very broad and indistinguishable. So, the effect is helpful in this way but can be unfavourable while interpreting the results. The enthalpy and entropy gained by fitting the dependencies in figure 5.12 are related only to the most flexible cooperative units of the network. And that is a problem because we can hardly say how many units are included in the measured signal.

If we try to compare the results of NMR table 5.3 and swelling experiments table 5.2, we find out the entropy and enthalpy are greater in table 5.3 for all samples. The problem with the signal from just a part of the cooperative domains could be one reason of that. The entropy and enthalpy from NMR spectra are relative only to the units visible in NMR spectra. These units are also "more active", go through more extensive change during the collapse than the less flexible and "invisible" domains. Hence, the studied quantities are greater than if it is relative to the whole sample like in the case of swelling experiments. The swelling experiments measurements are macroscopic, they take the whole sample and the result is an average of all the microscopic contributions.

If the amount and the length of the cooperative domains were known, the quantities could be recalculated to get a better correspondence. Unfortunately, the precisely structure of the sample is unknown and even having a microscopical picture of the hydrogel network structure, it would be very difficult to say which of the polymer chains are visible and what is the critical length. It might be a way how to fix the differences between the microscopic and macroscopic way of the measurement though.

Comparing quantities T_{on} and ΔT, these T_{on} gained from NMR are greater (approximately by 15 K) and ΔT shorter (by 5 to 10 K) than these of the swelling experiments. As it is already written, NMR is a microscopic method and the conformational change is much quicker on the microscopic level than macroscopic, at which some time for reaching the equilibrium is needed. It explains why the NMR critical temperature interval is shorter but it is shifted to higher temperature values in comparison with the swelling data.

The water split signal

Studying the samples NMR spectra, we found out that the water signal is split at PDEAAm/AAm system. The NMR spectra results are very sensitive on the heterogeneities of the magnetic field, which can be shown as the water signal split. After many measurement, the splitting persists. We can observe it only at PDEAAm/PAAm. These samples behave a bit differently than the other series at the NMR relaxations for example. The splitting may be connected with the heterogeneous, porous structure. The water molecules inside and outside the pores have a different chemical shift as their nearest environment is different. The porous and strongly heterogeneous structure is a feature differentiating the PDEAAm/PAAm from the SN and PDEAAm/PDMAAm anyway, so it could explain the water NMR signal splitting.

6.3 NMR - spin-spin relaxation time measurement

The water molecules dynamics in the hydrogel samples were studied using relaxation experiments and T_2 values are summarized in table 5.4.

The SN hydrogels are the only system at which a kind of bound water (values about 0.01 - 0.1 s) was recognized. The bound water seems to release above the critical temperature because its contribution is decreasing with time. Sample PDEAAm 3 have a bit different behaviour than 1 and 5. There is an extremely short time 24 h after collapse with a great contribution. We cannot precisely say what is the reason but it could be caused by oscillations of temperature during the measurement.

At the DN hydrogels, there is no bound water definitely. There is an exception at sample PDEAAm/PAAm 5 though. An extremely short relaxation time appears above the critical temperature. As mentioned, the deflections can be caused by the temperature oscillations during the measurement, when a temperature unit of the spectrometer lost the stability. Apart from that sample, no bound water at DN systems is observed. At PDEAAm/PAAm samples, a relaxation time about 1 s appears, which may be assigned to originally flexible water contained in a more hydrophilic part or pores of the hydrogel network and binds to the collapsed units above the critical temperature. The DN hydrogels with PAAm seem to be heterogeneous system with a porous structure.

The DN systems with PDMAAm have one major T_2 in all situations, below and above the collapse. These samples swell a lot but do not bond the water as the SN systems. The network probably creates a matrix for the water molecules, which are very weakly attracted but do not bind and stay very flexible acting as a free water. PDEAAm/PAAm are more heterogeneous systems than PDEAAm/PDMAAm, at which the porous structure is not revealed from the relaxation experiments.

6.4 UV-Vis spectroscopy

The UV-Vis experiments showed that a model solution is released exponentially during the collapse at all sample. Only PDEAAm 5 have a very fast collapse that the experimental arrangement did not enable to measure it. This sample reports an interesting feature though, see figure 5.19. After the collapse, released MB is bound back to the structure of the hydrogel. This feature was observed also at other samples at the end of the measuring but it was most significant at PDEAAm 5. There is probably a "critical time" after which hydrophobic MB bonds to the hydrogel network which has become more hydrophobic after the conformation change. The hydrophobic character of MB is a disadvantage at the drug releasing experiments. MB is partly hydrophobic as well as hydrophilic and the methyl groups and aromatic circles bind to the hydrophobic collapsed hydrogel. It depends on a character of the potential drug, only for the one with a similar rate of hydrophobicity, MB suitable as a model substance. More hydrophilic model solution would have definitely different properties and the behaviour after the collapse would be qualitatively different for sure.

The releasing experiments also showed us that there is a big difference between the SN and DN systems. In table 5.5, the SN hydrogels have a much longer time of the release but can carry more of the drug as they swell more. On the other hand, the DN hydrogels release is very quick, so it depends on the certain application which property is desired.

Conclusion

In this thesis, the temperature-sensitive PDEAAm was used for the SN and DN hydrogels preparation. The hydrogel networks of six different cross-linking density were prepared. The DN hydrogels were prepared in two series, each of them contained a different hydrophilic second component (PAAm, PDMAAm).

The basic properties and behaviour of the samples during the collapse were examined with the swelling experiments and also with the NMR spectroscopy techniques. We measured the parameters of the collapse for all samples but we found out that the samples properties are well proportional to the cross-linking density, so we properly investigated only three cross-linking density of each series, which was sufficient to characterise the samples behaviour.

The dynamics of the water molecules in the hydrogel before and after the collapse were studied with the NMR relaxation measurements. The character of water bonding change was described during the collapse. The methylene blue solution was used as a model solution for the drug release experiments. The releasing process in a hydrogel after the collapse was detected with UV-Vis spectrometer measuring the concentration of methylene blue in the hydrogel surrounding water solution.

One of the main results is that the second and hydrophilic component causes the broader temperature interval and decreases the extent (enthalpy and entropy) of the collapse, so it is not as significant as in the case of single network hydrogels.

It was proved that the cross-linking density of the hydrogel networks does not affect the collapse, but it influences the final composition of the double network hydrogels during the preparation. The collapse is then the same at the single network samples with different cross-linking density but it is differentiating at the double networks of varying cross-linking density.

The spin-spin relaxation time measurements demonstrate bound water existence only in the single network systems. The double network systems are probably heterogeneous, expecially PDEAAm/PAAm samples have a strongly porous structure.

Measuring drug model release, the exponential decay of the swollen solution in the hydrogel was proved. The hydrophobic methylene blue character that causes the attraction to the collapsed hydrogel showed that the solution release out of the amphiphilic polymer network is strongly influenced by the character of the solution. The experiments also showed that there is a limit cross-linking density, which is not suitable for a use in this application. The studied samples have different properties and might be used in various cases as a drug transport matrix.

List of abbreviation

- SN ..... single network
- DN ..... double network
- PAAm ..... polyacrylamide
- PDEAAm ..... poly(N, N'-diethylacrylamide)
- PDMAAm ..... poly(N, N'-dimethylacrylamide)
- PNIPAAm ..... poly(N-isopropyl acrylamide)
- AMPS ..... 2-acrylamido-2-methylpropane sulfonic acid
- TEMED ..... tetramethylethylenediamine
- OGA ..... oxoglutaric acid
- MBAAm ..... methylenebis(acrylamide)
- MB ..... methylene blue

Bibliography

[1] Naziha Chirani, L'Hocine Yahia, Lukas Gritsch, Federico Motta, Soumia Chirani, and Silvia Farè. History and applications of hydrogels. *Journal of Biomedical Sciences*, Vol. 4:13–23, 12 2015.

[2] Virginia Nykanen, Antti Nykänen, Mervi Puska, Glaura Silva, and Janne Ruokolainen. Dual-responsive and super absorbing thermally cross-linked hydrogel based on methacrylate substituted polyphosphazene. *Soft Matter*, pages 4414–4424, 05 2011.

[3] Wichterle. Hydrophilic gels for biological use. *Nature*, 185:117–118, 01 1960.

[4] Sytze J. Buwalda, Kristel Boere, Pieter J. Dijkstra, Jan Feijen, Tina Vermonden, and Wim Hennink. Hydrogels in a historical perspective: From simple networks to smart materials. *Journal of controlled release*, 190, 04 2014.

[5] John A. Hunt, Rui Chen, Theun van Veen, and Nicholas Bryan. Hydrogels for tissue engineering and regenerative medicine. *J. Mater. Chem. B*, 2:5319–5338, 2014.

[6] Xin Bai, Mingzhu Gao, Sahla Syed, Jerry Zhuang, Xiaoyang Xu, and Xue-Qing Zhang. Bioactive hydrogels for bone regeneration. *Bioactive Materials*, 3:401–417, 05 2018.

[7] Enrica Calò and Vitaliy Khutoryanskiy. Biomedical applications of hydrogels: A review of patents and commercial products. *European Polymer Journal*, 65, 04 2015.

[8] Shouei Fujishige and Isao Kubota, Kenji Ando. Phase transition of aqueous solutions of poly(*N*-ispropylacrylamide) and poly (*N*-isopropylmethacrylamide). *The Journal of Physical Chemistry*, 93, 04 1989.

[9] Jian Ping Gong, Takayuki Kurokawa, Tetsuharu Narita, Go Kagata, Yoshihito Osada, Goro Nishimura, and Masataka Kinjo. Synthesis of hydrogels with extremely low surface friction. *Journal of the American Chemical Society*, 123:5582–3, 07 2001.

[10] Jian Ping Gong. Why are double network hydrogels so tough? *Soft Matter*, 6, 06 2010.

[11] Xiaoyan Zhang, Xinglin Guo, Shuguang Yang, Shuaixia Tan, Xiaofeng Li, Hongjun Dai, Xiaolan Yu, Xiaoli Zhang, Ning Weng, Bin Jian, and Jian Xu. Double-network hydrogel with high mechanical strength prepared from two biocompatible polymers. *Journal of Applied Polymer Science*, 112:3063 – 3070, 06 2009.

[12] Hai Xin, Sureyya Zengin Saricilar, Hugh Brown, Philip Whitten, and Geoffrey Spinks. Effect of first network topology on the toughness of double network hydrogels. *Macromolecules*, 46:6613–6620, 10 2013.

[13] Ruochong Fei, Jason Thomas George, Jeehyun Park, and Melissa Grunlan. Thermoresponsive nanocomposite double network hydrogels. *Soft matter*, 8:481–487, 01 2012.

[14] Ruochong Fei, Jason T. George, Jeehyun Park, Kristen Means, and Melissa Grunlan. Ultra-strong thermoresponsive double network hydrogels. *Soft Matter*, 9:2912–2919, 02 2013.

[15] L. Kris Kostanski, Ruixiang Huang, Raja Ghosh, and Carlos Filipe. Biocompatible poly(*N*-vinyllactam)-based materials with environmentally-responsive permeability. *Journal of biomaterials science. Polymer edition*, 19:275–90, 02 2008.

[16] Thomas Baltes, Frédéric Garret-Flaudy, and Ruth Freitag. Investigation of the LCST of polyacrylamides as a function of molecular parameters and solvent composition. *Journal of Polymer Science Part A: Polymer Chemistry*, 37:2977 – 2989, 01 2000.

[17] Marilia Panayiotou, Claudia Pöhner, Caroline Vandevyver, Christine Wandrey, Frank Hilbrig, and Ruth Freitag. Synthesis and characterisation of thermo-responsive poly(*N,N'*-diethylacrylamide) microgels. *Reactive & Functional Polymers*, 67:807–819, 09 2007.

[18] Irene Idziak, Damien Avoce, David Lessard, D. B. Gravel, and Xiao Xia Zhu. Thermosensitivity of aqueous solutions of poly(*N,N'*-diethylacrylamide). *Macromolecules*, 32:1260–1263, 1999.

[19] Marilia Panayiotou and Ruth Freitag. Synthesis and characterisation of stimuli-responsive poly(*N,N'*-diethylacrylamide) hydrogels. *Polymer*, 46:615–621, 01 2005.

[20] Yasushi Maeda and Masato Yamabe. A unique phase behavior of random copolymer of *N*-isopropylacrylamide and *N,N'*-diethylacrylamide in water. *Polymer*, 50:519–523, 01 2009.

[21] Jude Ngadaonye, Luke Geever, Martin Cloonan, and Clement Higginbotham. Photopolymerised thermo-responsive poly(*N,N*-diethylacrylamide)-based copolymer hydrogels for potential drug delivery applications. *Journal of Polymer Research*, 19, 03 2012.

[22] Harald Günther. *NMR Spectroscopy - Basic Principles, Concepts, and Applications in Chemistry*. 09 2013.

[23] Lenka Hanyková, Jiří Spěváček, Marek Radecki, Alexander Zhigunov, Julie Šťastná, Helena Valentova, and Zdenka Sedlakova. Structures and interactions in collapsed hydrogels of thermoresponsive interpenetrating polymer networks. *Colloid and Polymer Science*, 293:709–720, 03 2014.

[24] Ivan Krakovský, Hana Kourilova, Martin Hrubovský, Jan Labuta, and Lenka Hanyková. Thermoresponsive double network hydrogels composed of poly(*N*-isopropylacrylamide) and polyacrylamide. *European Polymer Journal*, 116, 04 2019.

[25] B. Maheswari, P.E. Jagadeesh Babu, and Mayank Agarwal. Role of *N*-vinyl-2-pyrrolidinone on the thermoresponsive behavior of PNIPAm hydrogel and its release kinetics using dye and vitamin-B12 as model drug. *Journal of Biomaterials Science, Polymer Edition*, 25(3):269–286, 2014.

List of Figures

1.1 Hydrogel sample dried out (left) and swollen (right), [2] 4
1.2 Model of polymer network swollen in water 4
1.3 Plant cultivated with hydrogel beans 7
1.4 Hydrogel as extracellular matrix for cell cultivation, [5] 8
1.5 Bone regeneration of rat cranial deffect with and without hydrogel 12 weeks post-transplantation , [6] 8
1.6 Structure change of free chains - globules inducting collapse . . . 9

2.1 ^{1}H spectrum of poly(N, N'-diethylacrylamide) 13
2.2 Model of magnetization in magnetic field B_0 14
2.3 Proton chemical shift of function groups from organic solvents, [22] 16
2.4 The CPMG sequence for T_2 measuring 16

4.1 Poly($N, N^{'}$-diethylacrylamide) (PDEAAm) 19
4.2 Polymerized MBAAm 19
4.3 Model of double network formation 20
4.4 Poly(acrylamide) (PAAm) 20
4.5 Poly($N, N^{'}$-dimethylacrylamide) (PDMAAm) 21

5.1 Hydrogel before (left) and after (right) heating in the phial 23
5.2 Water molecules in networks of different cross-linking density . . . 24
5.3 Polymer fraction mass temperature dependency for SN hydrogels 25
5.4 Polymer fraction mass temperature dependency for DN/AAm hydrogels 25
5.5 Polymer fraction mass temperature dependency for DN/DMAAm hydrogels 26
5.6 Sample NMR 27
5.7 A section of NMR spectra PDEAAm/PAAm, measured with growing temperature 27
5.8 NMR spectrum of PDEAAm at 298 K 28
5.9 NMR spectrum of PDEAAm/PAAm at 298 K 29
5.10 NMR spectrum of PDEAAm at 327 K 30
5.11 NMR spectrum of PDEAAm/PAAm at 327 K 30
5.12 p-factor temperature dependency for the highest cross-linking density (1) of SN, DN with PAAm and PDMAAm 31
5.13 Time dependency of signal intensity 33
5.14 Chemical structure of MB 35
5.15 Hydrogel swollen in MB solution 35
5.16 Collapsed SN hydrogels originally swollen in MB solution (from left PDEAAm 1, PDEAAm 3, PDEAAm 5) 36
5.17 Collapsed PDEAAm 1 originally swollen in MB solution 36
5.18 UV-Vis spectra of MB measured after various time periods from immersion the hydrogel DN PDMAAm 1 in the phial 37
5.19 Time dependency of MB concentration for releasing process from SN hydrogels 38

5.20 Time dependency of MB concentration for releasing process from DN PAAm hydrogels 39
5.21 Time dependency of MB concentration for releasing process from DN PDMAAm hydrogels 39

List of Tables

4.1 Mass of MBAAm in the samples 20
4.2 Prepared samples 21

5.1 Intial mass fraction of polymer 23
5.2 Fitting parameters of w_p temperature dependency 24
5.3 Fitting parameters of p-factor temperature dependency 32
5.4 Spin-spin relaxation times of water in samples 34
5.5 Fitting parameters of MB concentration time dependency 40
5.6 Fractions $f(MB)$ of released MB from all studied hydrogels originally MB swollen 40